

Bayesian Optimization in Language space: An Eval-Efficient AI Self-Improvement Framework

Enoch Hyunwook Kang*

Foster School of Business, University of Washington

Hema Yoganarasimhan

Foster School of Business, University of Washington

November 18, 2025

Abstract

Large Language Models (LLMs) have recently enabled self-improving AI, i.e., AI that iteratively generates, evaluates, and refine its own outcomes. Recent studies have shown that self-improving AI focusing on prompt optimization (i.e., context engineering) can outperform state-of-the-art reinforcement-learning fine-tuned LLMs. Here, their ‘performance’ is typically measured by query efficiency—the number of LLM-generated solution samples required to reach a specified performance threshold. However, in many societal applications, the primary limitation is not *generating* new solutions but *evaluating* them. For instance, evaluating an ad’s effectiveness requires significant human feedback, which is far more costly and time-consuming than generating a candidate ad. To optimize for the evaluation efficiency objective, a natural approach is to extend Bayesian Optimization (BO), a framework proven optimal for evaluation efficiency, to the language domain. However, the difficulty of directly estimating suitable acquisition functions in LLMs’ minds makes this extension challenging. This paper overcomes this challenge by proving that the combination of the simple and widely used BEST-OF-N selection strategy and simple textual gradients (i.e., textual edits from a critic model) statistically emulates the behavior of the gradients on the canonical Upper Confidence Bound (UCB) acquisition function, which induces optimal exploration in terms of evaluation efficiency. Based on this result, we propose TEXTGRAD-BEST-OF-N BAYESIAN OPTIMIZATION (T-BoN BO), a simple and eval-efficient language-space Bayesian optimization framework for AI self-improvement. We also empirically validate T-BoN BO by applying it to automated ad alignment tasks for persona distribution, demonstrating its superior performance compared to popular state-of-the-art baselines. In sum, T-BoN BO is a simple but principled framework for AI self-improving system design that bridges prompt optimization with classical Bayesian optimization.

Keywords: Self-improving AI, Evaluation efficiency, Bayesian optimization, Context Engineering

*Please ask all correspondence to: ehwkang@uw.edu and hemay@uw.edu.

1 Introduction

1.1 Self-improving AI

Data-centric decision making has long relied on a human-driven cycle of historical data analysis, solution proposal, and experimentation. This human-driven iterative approach has supported a wide range of business decisions, ranging from website design [Hauser et al., 2009] to product recommendations [Nandy et al., 2021]. We briefly describe this paradigm using the example of ad-optimization; see the left panel of Figure 1. The process starts with a manager generating a set of ad creatives based on a creative brief. This task is often done by ad agencies or marketers, who rely on their understanding of the product, theories of consumer behavior, market conditions, and feedback from prior ad campaigns. This ad *generation* process typically takes weeks, and serves as the main bottleneck in the iterative ad-optimization process. Once we have a set of candidate ads, the manager moves to *evaluation*, i.e., feeds these ads into advertising platforms or consumer surveys to identify the best performing one, and this step usually takes a few days. Finally, to complete this feedback loop, the manager *analyzes* the performance of the ads from this campaign and uses the insights learned to generate a new slate of candidate ads; and the iterative process continues.

Although effective in many settings, this human-driven workflow suffers from drawbacks. First, the speed with which firms can iterate over this process depends critically on how *quickly* humans can learn from the performance of prior solutions and propose new candidate solutions. Historically, generating new candidate solutions (or ads in the case of our example) has been time-consuming, and this step formed a key bottleneck in speeding up the process. Further, there exists no formal framework for how human agents can learn from the performance of prior solutions and leverage them to propose better candidates, and this step is often left to managerial intuition. Indeed, much of the research and managerial focus on data-driven business solutions has largely centered on the *evaluation* step, i.e., given a set of candidate solutions/options, how can we identify the most effective one – and solutions such as A/B tests and Multi-Armed Bandits (MAB) experiments have been proposed and tested [Kohavi et al., 2020, Fiez et al., 2024]; but how to leverage insights from prior rounds of evaluation systematically and improve the set of candidate solutions remains an unsolved problem.

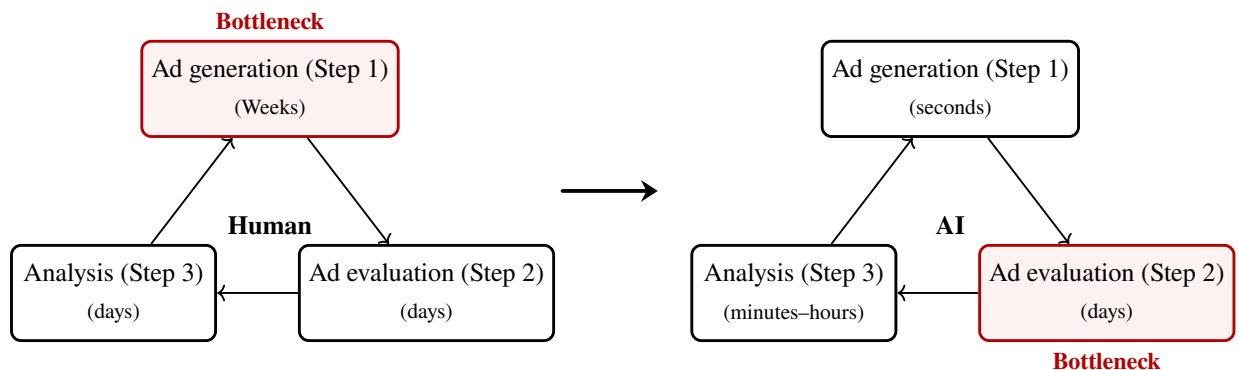


Figure 1: Comparison of human-driven and AI-driven ad self-improvement cycles in digital advertising.

Recent advances in generative AI have begun to transform this human-driven paradigm by providing

potential solutions to the issues discussed above. First, candidate generation is fast and scalable with generative AI models. For example, in the case of digital ads, generative models can produce high-quality creative outputs, including ad copy, images, and complete campaign concepts that adhere to brand guidelines in a matter of minutes [Jansen et al., 2024, Hartmann et al., 2025] (see right panel of Figure 1).¹ Second, Large language Models (LLMs) and related generative systems can now conduct sophisticated data analysis, summarizing performance patterns and identifying potential drivers of success [Ferber et al., 2024, Guo et al., 2024, Ghosh et al., 2024, Wiedemer et al., 2025], providing a pathway for analyzing historical data and improving candidate solutions. As such, with the new capabilities enabled by AI, the traditional bottlenecks of analysis and generation of candidate solutions are significantly reduced. Given these developments, there is immense interest in the development and deployment of *self-improving AI* [Silver and Sutton, 2025], which automates the complete analysis–generation–evaluation loop at scale, allowing systems to update themselves continuously in response to emerging data [Mantia et al., 2025, Chen et al., 2025].

1.2 Research Agenda and Challenges

In this paper, we study a prompt-optimization-based self-improving AI framework for societal and business problems, motivated by recent successes of prompt-optimization-based self-improving AI algorithms that outperform state-of-the-art reinforcement learning fine-tuning methods [Agrawal et al., 2025]. While the use of modern generative AI systems has reduced the overhead associated with content generation and analysis (Steps 1 and 3), there are still three challenges that we need to overcome to design an efficient and effective self-improving AI that can automate decision-making in societal and business problems.

- Challenge 1 – Evaluation-efficiency

First, in many real-world societal and business problems, the primary bottleneck is no longer *generating* new solutions efficiently (query efficiency) but *evaluating* them efficiently (evaluation efficiency). For instance, in the case of digital advertising, generating ad creatives using LLM queries is super fast, but evaluating an ad’s effectiveness requires significant human feedback or large-scale experimentation [Johnson, 2023]. As such, any AI system that we design needs to be *evaluation-efficient*, i.e., reach a high-performing solution using as few costly evaluations as possible, rather than trying to optimize for a few inexpensive generations as possible. While there is a nascent but growing literature in computer science on self-improving AI systems, this literature mainly focuses on generation efficiency as the main bottleneck [Agrawal et al., 2025], and has largely overlooked evaluation efficiency.

- Challenge 2 – Lack of gradient functions

Second, notice that we are essentially solving an optimization problem in language space, i.e., we want to take an input prompt, evaluate its performance, and improve it to reach a higher performance.² In standard numerical settings, the natural way to solve such problems is to use gradient functions. However,

¹Indeed, a substantial share of creatives is now generated by AI, reflecting improvements in both quality and speed [Coffee, 2025, Majic, 2025].

²Self-improving AI can thus be viewed as principled prompt optimization or context engineering since it involves improving textual inputs/prompts based on historic performance data [Zhou et al., 2022, Khattab et al., 2023, Yang et al., 2024, Yuksekogonul et al., 2025, Agrawal et al., 2025, Zhang et al., 2025, Wang et al., 2025].

in language spaces, the notion of a gradient is ill-defined because they lack the inner-product structure of a Hilbert space required to measure the directions and magnitudes of change [Young, 1988]. Thus, we first need to define a meaningful notion of a “gradient” in the domain of text.

- **Challenge 3 – Balancing exploration and exploitation**

Third, while it is tempting to move fully along the textual gradient that worked well previously, i.e., *exploit* the knowledge gained from prior prompts, this can be sub-optimal due to uncertainty about that knowledge. Thus, we also need to bake some *exploration* in the choice of gradient direction. Again, while there exist bandit-based approaches that balance exploration and exploitation in the case where we have a fixed candidate set and the exploration space is numerical [Jamieson and Nowak, 2014, Russo, 2016, Russo et al., 2018, Mason et al., 2020, Simchi-Levi and Wang, 2023, Fiez et al., 2024], these do not automatically translate to our setting since our goal is to explore in the language space and our exploration focuses on *changing* the set of candidate solutions rather than deciding how much to explore each option within a fixed candidate set. Thus, a key challenge is to account for uncertainty to guide the search over the language space. Canonical uncertainty measures, such as the Upper Confidence Bound (UCB) or the posterior distribution, are not readily available from off-the-shelf LLMs, making their direct application to language space non-trivial. Further, we note that self-consistency variance or embedding distances are poor proxies, and training a Gaussian Process over high-dimensional text embeddings is brittle, difficult to implement, expensive, and data-hungry.

In this paper, our goal is to address the above challenges and build an evaluation-efficient self-improving AI that effectively balances exploration and exploitation in the language space.

1.3 Our Framework and Algorithm

We start with the observation that prompt optimization for self-improving AI follows a familiar pattern – we iteratively choose a candidate prompt that generates a candidate solution, observe a noisy performance score associated with this solution, and then decide where to query next while minimizing evaluations. Throughout, we have to be cognizant of three concerns: (1) we need to balance exploration and exploitation when choosing the next candidate solution, (2) we have no closed-form model linking prompts to scores, and (3) the main scarce resource is the number of evaluations rather than candidate generation. Our key insight is that these features of our problem are similar to the regime in which classic *Bayesian Optimization (BO)* operates successfully [Frazier, 2018, Srinivas et al., 2012, Papenmeier et al., 2025]. BO is a principled framework for tackling black-box optimization problems where evaluation efficiency is an important consideration. (See Web Appendix E for a detailed theoretical discussion of BO.) Thus, we seek to extend BO from numerical inputs to the space of natural language prompts to design an evaluation-efficient self-improving AI.

At its core, BO assumes a *surrogate model* (e.g., Gaussian Process or Reproducing Hilbert Kernel Space) to approximate the objective function and provide uncertainty estimates of that approximation. From this surrogate, BO constructs a function often called the *acquisition function* and selects as the next candidate the point with the highest acquisition value. One of the most widely used BO methods is Bayesian Optimization with Upper Confidence Bound (UCB) acquisition function [Srinivas et al., 2012]. In practice, since the

global maximizer of the UCB acquisition function is often not available in a closed form, we typically use gradient-based BO with UCB acquisition function [Wilson et al., 2018]. Gradient-based BO methods have shown surprising effectiveness for high-dimensional problems when the gradient-based BO is adapted to avoid vanishing gradients, for example, through random multi-start (where each initialization yields a local maximum of UCB) and careful gradient sampling strategies [Papenmeier et al., 2025]. However, the standard gradient-based UCB BO is not directly applicable to the language space, as the notion of a gradient is ill-defined because they lack the inner-product structure of a Hilbert space required to measure the directions and magnitudes of change [Young, 1988]. Therefore, we first need to define a notion of gradients in the language space and devise an appropriate acquisition function in the text space.

We now describe how we modify and adapt the BO framework to address the challenges discussed earlier. We propose a simple, evaluation-efficient iterative prompt-optimization framework that we call `TEXTGRAD-BEST-OF-N BAYESIAN OPTIMIZATION` (T-BoN BO) that addresses all three challenges discussed earlier. First, the BO framework naturally addresses the first challenge of the evaluation efficiency. It is known that BO with UCB acquisition function [Srinivas et al., 2012] is a theoretically evaluation-efficient algorithm, i.e., optimally balances exploration and exploitation, minimizing regret [Whitehouse et al., 2023, Wang et al., 2023]. Specifically, for both expected cumulative regret and simple regret, the regret upper bound of BO with UCB acquisition function tightly matches the regret lower bound of Scarlett et al. [2017].

To solve the second challenge, T-BoN BO builds on the recently proposed `TEXTGRAD` [Yuksekgonul et al., 2025] framework that adapt gradient descent to discrete text by asking an external auxiliary LLM *critic* to propose targeted edits that improve a candidate; applying these edits induces a local, directional update, i.e., a “textual gradient”, in language space. This makes gradient-style search feasible without continuous relaxations or mapping the LLM prompts to the embedding space. Yuksekgonul et al. [2025] show that textual gradients based on their approach enable consistent improvements across diverse scientific domains such as code-completion benchmarks, improving accuracy on graduate-level QA datasets, optimizing drug-like molecules, and refining radiotherapy planning for clinical objectives. These results establish textual gradients as an effective surrogate for numerical gradients when optimizing systems that operate in language space.

To address the third challenge, T-BoN BO chooses the next prompt to evaluate via a series of textual gradients which are selected under the Best-of- N principle [Snell et al., 2024]. Moving in the textual gradient direction suggested by the critic exploits the expected improvement implied by past results but ignores uncertainty in those expectations. T-BoN bakes in *exploration* into the choice of gradient direction by adopting an optimism-based rule in the spirit of the optimism-in-the-face-of-uncertainty principle: it samples multiple local textual edits and moves along the direction the LLM judges most promising, i.e., the Best-of- N candidate. We show that Best-of- N over locally sampled textual edits statistically emulates gradient ascent on a UCB acquisition function, so that Best-of- N effectively acts as an implicit optimistic acquisition maximizer in language space.

We now briefly describe our T-BoN BO algorithm. At each optimization iteration, in Step 1 (meta-reflection phase), we use the critic model to analyze the history of previously evaluated solutions and their

scores, and update a meta-reflection that summarizes what has tended to work well or poorly. In Step 2 (Best-of- N textual-gradient phase), we perform a sequence of textual gradient updates: for each gradient step, (i) we propose N textual-gradient edits that transform the current prompt into N candidate prompts, (ii) each candidate prompt is passed to a solution-generation model to produce a corresponding candidate solution, (iii) conditioned on the meta-reflections, the critic model predicts which candidate solution is most likely to perform best, and (iv) we set the prompt associated with this predicted-best solution as the new current prompt. After iterating Step 2, we obtain a refined prompt and its associated solution to evaluate. In Step 3 (evaluation phase), we evaluate this solution to obtain a scalar score, which is then used by T-BoN BO to update its history and meta-reflection for subsequent optimization steps.

1.4 Theoretical Guarantees and Empirical Evaluation

We provide theoretical guarantees on the performance of our approach. We formally show that, under mild regularity conditions, the Best-of- N selection over locally sampled textual edits induces, in probability, ascent directions of the UCB acquisition function with an exploration parameter $\beta_N = \Theta(\sqrt{\ln N})$ (Theorem 2). In other words, T-BoN BO emulates gradient-based UCB Bayesian Optimization in the implicit embedding space induced by the LLM, even though it operates purely in language space and does not construct an explicit surrogate or uncertainty model. Since UCB-BO is known to achieve sublinear regret and optimal evaluation-efficiency guarantees, T-BoN BO inherits these theoretical properties up to constant factors and approximation error stemming from textual gradients. In sum, we formally establish that T-BoN BO is theoretically equivalent to the gradient-based implementation of Bayesian Optimization with the Upper Confidence Bound (UCB) acquisition function [Srinivas et al., 2012, Wilson et al., 2018], which is proven to be evaluation-efficient [Whitehouse et al., 2023, Wang et al., 2023]. This equivalence establishes T-BoN BO as a valid, eval-efficient, gradient-based Bayesian optimization procedure in the language space.

In addition to its theoretical efficiency, T-BoN BO is simple and easy to implement since does not require any explicit uncertainty modeling, embeddings, or Gaussian process surrogates. We now demonstrate the empirical performance of our approach using a series of numerical experiments. Concretely, we instantiate T-BoN BO in a digital advertising setting, where the goal is to iteratively refine image-generation prompts for ad creatives so as to maximize ad responsiveness for a population of customers. We test and measure how well and how fast a method optimizes for (i.e., aligns with) the preference distribution induced by LLM-based simulation of personas in the Digital Twins persona dataset called Twin-2k-500 [Toubia et al., 2025].³ We demonstrate that T-BoN BO significantly outperforms strong state-of-the-art baselines such as BEST-OF-N [Snell et al., 2024] and GEPA [Agrawal et al., 2025] in terms of evaluation efficiency, i.e., reaching fixed performance with a smaller number of steps. Specifically, we show that:

- T-BoN BO, the proposed evaluation efficient framework, achieves nearly twice more improvements from BEST-OF-N baselines compared to GEPA [Agrawal et al., 2025], the state-of-the-art prompt optimization-

³While LLM-based persona simulation can be biased and may not reflect real-world human behavior [Li et al., 2025a, Peng et al., 2025], it still induces a valid preference distribution. As such, it can serve as a valid benchmark on which we can compare the performance of different AI-based optimization methods.

based self-improving AI algorithm, which outperforms GRPO [Liu et al., 2024a], the state-of-the-art reinforcement learning fine-tuning algorithm.

- T-BoN BO outperforms the state-of-the-art baseline even when we simulate preferences without any persona information, i.e., when the evaluator is a single LLM judge with no auxiliary context.

Together, these results show that T-BoN BO can reach good performance both in settings where there is significant heterogeneity in the preferences of the target population as well as in settings with homogeneous preferences.

In sum, our paper makes four main contributions to the literature on AI, optimization, and data-driven decision making. First, from a conceptual perspective, we identify evaluation efficiency as the key objective to optimize in self-improving AI design in societal and business systems. Second, we propose T-BoN BO, a purely text-based self-improving AI framework that combines textual-gradient search with Best-of- N selection to automate and optimize business and marketing decisions (e.g., ad creatives, product descriptions). Third, we provide theory showing that Best-of- N over locally sampled textual edits selects, in probability, ascent directions of the UCB acquisition with exploration weight $\beta = \Theta(\sqrt{\ln N})$; thus, we prove that T-BoN BO emulates gradient-based UCB and inherits evaluation-efficiency guarantees. Finally, we demonstrate empirical gains on automated ad-alignment across eight scenarios: T-BoN BO improves faster and attains higher final scores compared to strong baselines, including BEST-OF-64 and GEPA, and remains effective both in settings with and without contextual information.

The rest of the paper is organized as follows. Section 2 discusses the related literature. Section 3 describes the preliminaries related to the ideas discussed in this paper. Section 4 formalizes the AI system and its objective, along with self-improving algorithms. Section 5 introduces the main algorithm proposed in this paper, T-BoN BO, and its components. Section 6 proves that T-BoN BO theoretically emulates the gradient-based UCB Bayesian Optimization. Sections 7 and 8 empirically demonstrate T-BoN BO’s effectiveness on ad-alignment tasks versus strong baselines. Finally, Section 9 concludes with a discussion of implications and limitations.

2 Related Literature

Our paper relates and contributes to multiple streams of literature, including the literature on AI and LLMs in computer science, the operations literature on optimization, and the marketing literature on ad optimization. We now discuss each one below.

The literature on self-improving AI systems has often been motivated by an observation: the progress in AI based only on human data is hitting limits, so AI systems must create and learn from their own data. In other words, powerful AI systems “should have their own stream of experience that progresses, like humans, over a long time-scale” [Silver and Sutton, 2025]. That is, we need to design the self-improving AI system that iteratively 1) generate data of outcomes, evaluate outcomes with grounded signals, and 2) self-tune the three knobs –*models*, *tools*, and *prompts*– in the system to achieve long-term objectives under real-world feedback [Wang et al., 2025]. Here, tuning models is about altering language models’ input-output correspondences [Huang et al., 2023, Lee et al., 2023, Acikgoz et al., 2025]; tuning tools is about specifying the tools the

AI system has access to, including memory tools [Hou et al., 2025, Ouyang et al., 2025, Qiu et al., 2025]; tuning prompts is about engineering prompts in the model’s context window, including system messages, task instructions, constraints, schemas, and few-shot exemplars [Zhou et al., 2022, Khattab et al., 2023, Yang et al., 2024, Yuksekogonul et al., 2025, Agrawal et al., 2025, Zhang et al., 2025, Wang et al., 2025].

In this paper, we study self-improving systems, focusing on tuning prompts, which have recently attracted attention after Agrawal et al. [2025] showed that iterative prompt optimization can be more efficient than state-of-the-art model fine-tuning techniques such as GRPO [Liu et al., 2024a]. Specifically, given any limited budget for the number of LLM generation query calls, their proposed iterative prompt optimization method, named GEPA (Genetic-Pareto), outperformed GRPO across their experiments. Those experiments included benchmarks such as complex questions across multiple Wikipedia articles, strict instruction-following under constraints, retrieval-augmented fact verification to support or refute claims, and maintaining answer quality while avoiding privacy leakage. In all those benchmarks, the number of LLM query calls for generating candidate answers was considered as the primary performance bottleneck. Likewise, prior literature on prompt-based self-improving AI [Agrawal et al., 2025, Zhang et al., 2025, Wang et al., 2025] has focused on measuring efficiency in terms of *generation efficiency*, i.e., minimizing the number of LLM-generated rollouts. On the other hand, our paper proposes and focuses on the *evaluation efficiency* objective. That is, instead of focusing on reducing the number of LLM outcome-generation rollouts, we aim to reduce the number of evaluations required to achieve an effective outcome.

Our paper also relates to the literature on relating LLMs to Bayesian Optimization (BO). A series of papers focuses on applying LLM to enhance BO for numerical optimization problems. Liu et al. [2024b] focuses on leveraging LLMs’ contextual understanding and few-shot learning capabilities to improve BO’s efficiency, enabling better warm-starting and surrogate modeling; Aglietti et al. [2025] uses an LLM to discover new acquisition functions for Bayesian optimization. The LLM writes candidate acquisition function formulas as code, which are evaluated on various optimization problems. Conversely, Singh et al. [2025] applies BO to enhance LLM’s internal behavior to boost the model’s zero-shot and few-shot performance. In contrast to these papers, our paper focuses on considering the prompt optimization problem that arises in LLM-based self-improving AI system design as a Bayesian Optimization problem. In line with this focus, Schneider et al. [2025] and Kong et al. [2025] formulate prompt optimization among the fixed set of candidate prompts as Bayesian optimization. While Schneider et al. [2025] utilizes ideas from adversarial bandits, Kong et al. [2025] feeds each prompt text into an embedding model, and the GP surrogate operates on those fixed embedding features to guide selection. In contrast to these approaches, our work focuses on self-improving AI systems that actively generate new candidate prompts as the process proceeds, rather than pre-specifying a fixed set of candidate prompts.

In terms of method evaluation benchmarks, our paper relates to the methodological literature on ad optimization in digital marketing. A series of papers focused on the efficient execution of ad evaluation, i.e., iteratively improving ad choice efficiently given a fixed set of candidate ads. Schwartz et al. [2017] adopts Thompson Sampling with a hierarchical general linear model for a real display advertising campaign for a

financial-services firm, which purchased display advertising across 59 websites. Geng et al. [2020] partitions JD.com’s platform users into disjoint sub-populations and applies a contextual Thompson sampling algorithm to maximize the expected advertiser payoff. Aramayo et al. [2023] developed a contextual Thompson sampling algorithm to dynamically determine the list of house ads to display on the homepage of an electronic retailer to maximize the accumulated click-through rate of the ads. Ba et al. [2022] used parametric Thompson Sampling, where a parametric structure links features (media, audience attributes) to conversion likelihood to optimally allocate ad-media and target-audience combinations in high-dimensional settings with low success rates. The main difference between bandit-based papers and ours is the existence of a pre-defined set of candidate arms. Self-improving AI systems focus on creating new solutions by analyzing previous results. On the other hand, bandit methods aim to balance exploration of a predefined set of candidate ads optimally. More broadly, there is also a difference in problem scope. Self-improving AI systems iterate among three steps: generation, evaluation, and analysis. In contrast, bandit methods focus on efficiently executing the evaluation step. Indeed, an AI self-improvement framework’s evaluation step may employ a bandit method to improve efficiency further.

3 Preliminaries

3.1 AI system.

An AI system Φ can be formally defined as a feed-forward *modular workflow*, which consists of one or more interconnected Large Language Model (LLM) components. In line with prior work [Soylu et al., 2024, Khattab et al., 2022, Opsahl-Ong et al., 2024, Tan et al., 2025, Agrawal et al., 2025], we define an AI system Φ as a tuple $(M, C, \mathcal{X}, \mathcal{Y})$. Here, $M = \langle M_1, \dots, M_{|M|} \rangle$ represents the set of LLM-powered components, C is the control logic that orchestrates the workflow and sequences the tasks, and \mathcal{X} and \mathcal{Y} define the system input space and the system output space. Each component $M_i = (\pi_i, \theta_i, \mathcal{I}_i, \mathcal{O}_i)$ is an independent unit where π_i is the prompt, θ_i represents the fixed weights of the underlying language model, and $\mathcal{I}_i, \mathcal{O}_i$ specify the component’s input space and output space.

We denote the prompts in the whole system $\Pi = \langle \pi_1, \dots, \pi_{|M|} \rangle$. As the prompts Π are what we system designers can control for the system Φ , we denote Φ as the functional $\Phi(\cdot)$ when we would like to emphasize system Φ ’s dependency on prompts Π . Accordingly, we call $\Phi(\Pi)$ the ‘system outcome’ corresponding to prompt Π . Note that $\Phi(\Pi)$ is itself a function that maps \mathcal{X} to \mathcal{Y} , i.e., $\Phi(\Pi) : \mathcal{X} \mapsto \mathcal{Y}$.

Figure 2 illustrates an example AI system with five LLM-powered components. Here, its control logic $C = \{\mathcal{X} \rightarrow \{M_1, M_2\}, M_1 \rightarrow M_3, M_2 \rightarrow M_4, \{M_3, M_4\} \rightarrow M_5 \rightarrow \mathcal{Y}\}$ describes that the the system input \mathcal{X} becomes the component input for M_1 and M_2 , M_3 ’s input is M_1 ’s output, M_4 ’s input is M_2 ’s output, M_5 ’s input is M_3 ’s output and M_4 ’s output, and the final output \mathcal{Y} is the output of M_5 . The system Φ ’s input is the prompt $\Pi = \langle \pi_1, \pi_2, \pi_3, \pi_4, \pi_5 \rangle$.

3.2 TEXTGRAD: Textual gradients in language space.

A central question for extending gradient-based Bayesian optimization to text is how to define a usable notion of “gradient” in language. A recent influential paper by [Yuksekgonul et al., 2025] addresses this

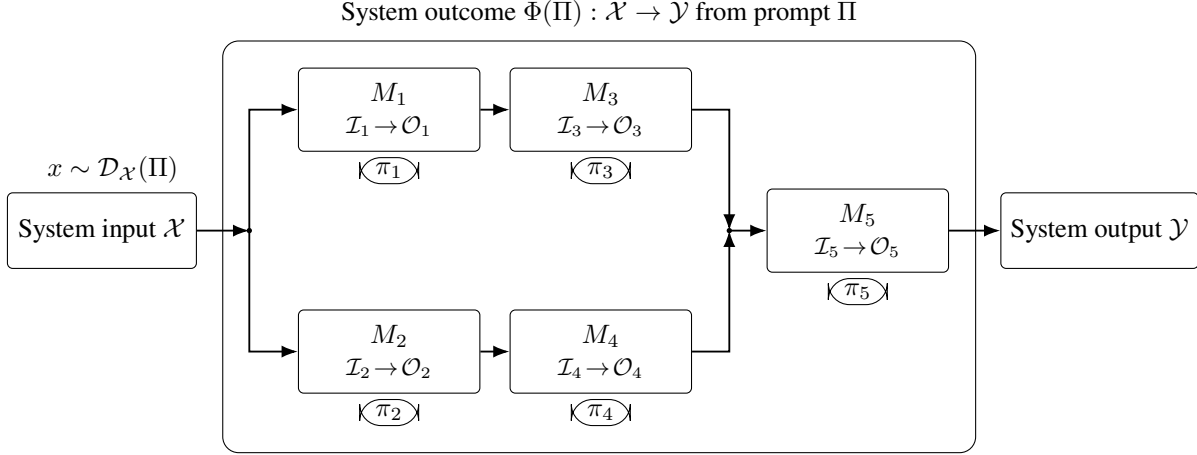


Figure 2: An example AI system with control logic $C = \{\mathcal{X} \rightarrow \{M_1, M_2\}, M_1 \rightarrow M_3, M_2 \rightarrow M_4, \{M_3, M_4\} \rightarrow M_5 \rightarrow \mathcal{Y}\}$ and prompt $\Pi = \langle \pi_1, \pi_2, \pi_3, \pi_4, \pi_5 \rangle$.

problem by proposing a framework called the `TEXTGRAD`; and it has attracted broad interest across multiple research communities. Instead of computing numerical derivatives, `TEXTGRAD` asks a critic LLM to propose targeted edits that would improve a candidate text. These edits act as local, directional signals, i.e., *textual gradients*, that guide search in a discrete language space. Importantly, this approach does not require embedding relaxations or external surrogate models, making it directly applicable to prompt optimization and other text-centric tasks.

For instance, consider an ad creative generation prompt for an image model: “A simple photo of a plant-based burger on a white plate.” A critic LLM might suggest: “Make the burger appear delicious, and show it being enjoyed at a barbecue.” Incorporating this edit yields: “A photorealistic image of a juicy plant-based burger with grill marks, served at a vibrant summer barbecue with friends.” This change is analogous to following a gradient direction—small, constructive, and aligned with improving performance according to the evaluation signal.

Empirical studies provided in Yuksekgonul et al. [2025] show that textual gradients enable consistent improvements across diverse scientific domains. In programming tasks, they raise success rates on challenging code-completion benchmarks. In knowledge-intensive reasoning, they improve accuracy on graduate-level QA datasets. In applied domains, they have been used to optimize drug-like molecules (via text encodings) and to refine radiotherapy planning prompts for clinical objectives. These results establish textual gradients as an effective surrogate for numerical gradients when optimizing systems that operate in and over language, justifying our use of gradient-style search in the discrete text space.

3.3 Bayesian Optimization.

Bayesian Optimization (BO) is a framework for maximizing an unknown and expensive-to-evaluate objective function under a limited evaluation budget. Formally, consider a black-box function $f : \mathcal{Z} \rightarrow \mathbb{R}$, where in our setting f corresponds to the system-level objective $J(\Pi)$ over prompts. BO maintains a *surrogate model*,

typically a Gaussian Process (GP) or another probabilistic regressor defined on \mathcal{Z} , that summarizes current beliefs about f . For any candidate $z \in \mathcal{Z}$, the surrogate yields a posterior mean $\mu(z)$ and an associated uncertainty measure $\sigma(z)$.

The next evaluation point is selected by maximizing an *acquisition function* $A(z)$ constructed from $\mu(z)$ and $\sigma(z)$, rather than by directly maximizing $\mu(z)$. Acquisition functions encode an explicit trade-off between *exploitation* (preferring points with high predicted value) and *exploration* (preferring points with high uncertainty). A widely used choice is the Upper Confidence Bound (UCB) acquisition function is:

$$A_\beta(z) = \mu(z) + \beta \sigma(z), \tag{1}$$

where the exploration parameter $\beta > 0$ controls the strength of the exploration term [Srinivas et al., 2012, Wilson et al., 2018]. In many applications, the maximizer of A_β is not available in closed form, and one instead employs *gradient-based BO*, which performs local ascent on A_β (often from multiple random initializations) to obtain approximate maximizers [Wilson et al., 2018, Papenmeier et al., 2025]. In gradient-based BO, each evaluation is followed by multiple gradient steps that identify local optima of the acquisition function. Gradient-based BO methods have shown surprising effectiveness for high-dimensional problems under random multi-starts and careful choice of gradients [Papenmeier et al., 2025].

In our setting, we do not construct an explicit surrogate model; rather, we interpret $\mu(\cdot)$ and $\sigma(\cdot)$ as implicit beliefs realized within the LLM and design our method to emulate the behavior of gradient-based UCB in this implicit space.

4 Overview of Self-Improving AI Algorithms

4.1 The optimization objective.

Consider a system designer’s decision making problem, where she chooses the prompt set Π for the LLM-based AI system Φ .⁴⁵ We call $\Phi(\Pi)$ the ‘system outcome’ of Φ corresponding to a prompt set Π . In a digital marketing setting, Φ is an image generation AI, and $\Phi(\Pi)$ is the ad generated by the prompt set Π . As a system, $\Phi(\Pi)$ has inputs and corresponding outputs. Specifically, $\Phi(\Pi)$ maps the input space \mathcal{X} to a distribution over an output space \mathcal{Y} . For each $x \in \mathcal{X}$, we denote by $y(\Phi(\Pi), x)$ the random \mathcal{Y} -valued vector output of the system at input x . In a digital marketing setting, input $x \in \mathcal{X}$ is a platform user, and a realization of $y(\Phi(\Pi), x)$ represents that user’s reaction (e.g., clicks, conversions, spend) to the ad $\Phi(\Pi)$.

The distribution of inputs over \mathcal{X} may depend on the prompts set Π . For example, in a digital marketing setting, a recommender system on the ad platform determines which users are shown the ad $\Phi(\Pi)$. To capture such dependences, we denote the input distribution over \mathcal{X} by $\mathcal{D}_\mathcal{X}(\Pi)$.

To evaluate the output, we use a scoring rule: a function $r : \mathcal{Y} \rightarrow [0, 1]$ that assigns a scalar effectiveness score to each $y \in \mathcal{Y}$. In the digital marketing example, r is a marketer-defined function that maps observed

⁴We call Π in a plural form ‘prompts’ or ‘prompt set’ instead of a singular form ‘prompt’, as there are often multiple prompt components in one system. See AI system paragraph in Section 3.1 for a detailed description of an AI system.

⁵LLM-based AI systems can also be modified by tuning the LLM’s internal parameters using LLM fine-tuning methods such as GRPO [Liu et al., 2024a]. In this paper, we focus on prompt optimization, which fixes those internal parameters throughout.

user responses (clicks, conversions, spend) to a normalized scalar effectiveness score.

Our optimization objective is to discover the prompt Π^* that maximizes the objective function

$$J(\Pi) := \mathbb{E}[r(y(\Phi(\Pi), x))]. \quad (2)$$

Note that J cannot be optimized by directly computing gradients, because the input distribution $\mathcal{D}_{\mathcal{X}}(\Pi)$ can shift with Π ; even when $J(\Pi)$ is differentiable with respect to Π and y 's randomness is not dependent on Π , we have:

$$\nabla_{\Pi} J(\Pi) = \underbrace{\mathbb{E}[\nabla_{\Pi} r(y(\Phi(\Pi), x))]}_{\text{model term}} + \underbrace{\mathbb{E}[r(y(\Phi(\Pi), x)) \nabla_{\Pi} \log d_{\Pi}(x)]}_{\text{distribution term}}, \quad (3)$$

where d_{Π} is the density of $\mathcal{D}_{\mathcal{X}}(\Pi)$. Since d_{Π} and $\nabla_{\Pi} \log d_{\Pi}(x)$ are unobservable, we cannot compute gradients from observed rewards. This motivates the use of an external LLM that can analyze prior data and propose directions for improvement without explicitly computing gradients, leading to self-improving AI algorithms we describe below that iteratively optimize for J .

4.2 Critic LLM and Self-improving AI algorithm

Given a scoring rule r , a *self-improving AI algorithm* \mathcal{A} optimizes $J(\Pi)$ through iteratively analyzing the previous history, proposing new prompts, and observing their scores. This is often enabled by assuming an external *critic LLM*, denoted M_{critic} , that can analyze previous data and propose the next solution.

Critic LLM. Specifically, a critic LLM is assumed to have the following capabilities:

- 1) The critic LLM can look at $\Phi(\Pi_1)$ and $\Phi(\Pi_2)$ side by side and predict which one will be better.
- 2) The critic LLM can read the history of past attempts and summarize the main lessons as a short list of rules or guidelines.
- 3) The critic LLM can suggest a small set of prompt edits that are likely to improve the current prompt.

In the digital-marketing example, these correspond to an LLM's ability to (1) compare two ad creatives and predict which will perform better [Calderon et al., 2025], (2) examine past performance data and derive guidelines for effective ads in context [Jiang et al., 2024, Ferber et al., 2024], and (3) propose prompt improvements based on those guidelines [Yuksekgonul et al., 2025, Li et al., 2025b].

Self-improving AI algorithm Given an initial prompt defined as Π_0 , a self-improving AI algorithm proceeds in discrete optimization iterations, indexed by $t = 1, 2, \dots$. At the beginning of iteration t , the algorithm has access to the history of past prompts and their observed scores and then selects a new prompt set Π_t , deploys the corresponding system $\Phi(\Pi_t)$, and receives feedback about its performance. At each algorithm iteration t , we define the score s_t of prompts Π_t as the empirical average reward at t , i.e.,

$$s_t := \frac{1}{L} \sum_{l=1}^L r(y(\Phi(\Pi_t), x_t^{(l)})), \quad x_t^{(l)} \sim \mathcal{D}_{\mathcal{X}}(\Pi_t), \quad (4)$$

where L denotes the number of input samples of $x_t^{(l)}$ we evaluate for each t . Note that we compare the performance of algorithms in terms of the progress of s_t across iterations t .

Given access to a history of past evaluations $H_{t-1} = \{(\Pi_\tau, s_\tau)\}_{\tau=1}^{t-1}$ where s_τ is the empirically evaluated score for the prompts Π_τ , a *self-improving AI algorithm* is defined as an algorithm \mathcal{A} iterates the following steps at each t to optimize for $J(\Pi)$:

1. **Analysis:** The critic LLM analyzes the previous history H_{t-1} .
2. **Generation:** The critic LLM proposes the next prompts Π_t based on the analysis.
3. **Evaluation:** The system $\Phi(\Pi_t)$ is deployed, and its performance is measured, yielding a score s_t . The new observation is added to the history: $H_t = H_{t-1} \cup \{(\Pi_t, s_t)\}$.

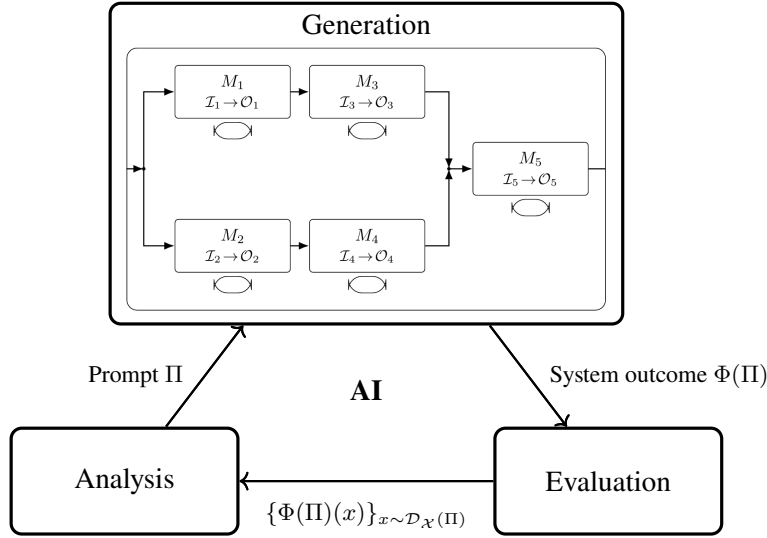


Figure 3: A self-improving AI algorithm implemented on the example AI system in Figure 2.

Figure 3 illustrates how the example AI system described in Figure 2 is positioned in the self-improving AI.

5 TextGrad-Best-of-N Bayesian Optimization (T-BoN BO)

We now describe the self-improving AI framework proposed in this paper, **TEXTGRAD-BEST-OF-N BAYESIAN OPTIMIZATION (T-BoN BO)** (Algorithm 1). Along with the system to optimize Φ and the scoring rule r , it requires a critic model M_{critic} .

Algorithm. T-BoN BO starts from an initial prompt Π_0 . Initially at iteration $t = 0$, it gets the initial system $c_0 = \Phi(\Pi_0)$ and evaluates it on $\mathcal{D}_{\mathcal{X}}(\Pi_0)$ to obtain initial score $s_0 = \text{Eval}(c_0, \mathcal{D}_{\mathcal{X}}(\Pi_0))$. The history and the reflection is initialized as $H_0 = \{(\Pi_0, c_0, s_0)\}$ and $R_0 = \emptyset$.

We first fix the hyperparameters: the number of candidates per gradient step (N), the number of gradient steps per iteration (G), and the number of iterations (T). Then at each iteration t , it first sets $\Pi_{t,0}$ as Π_{t-1} , the previous iteration’s prompt, and proceeds as follows:

1. **Best-of-N Textual Gradient steps.** (Detailed in Section 5.1) Repeat steps 1) – 4) for $g = 1, \dots, G$:

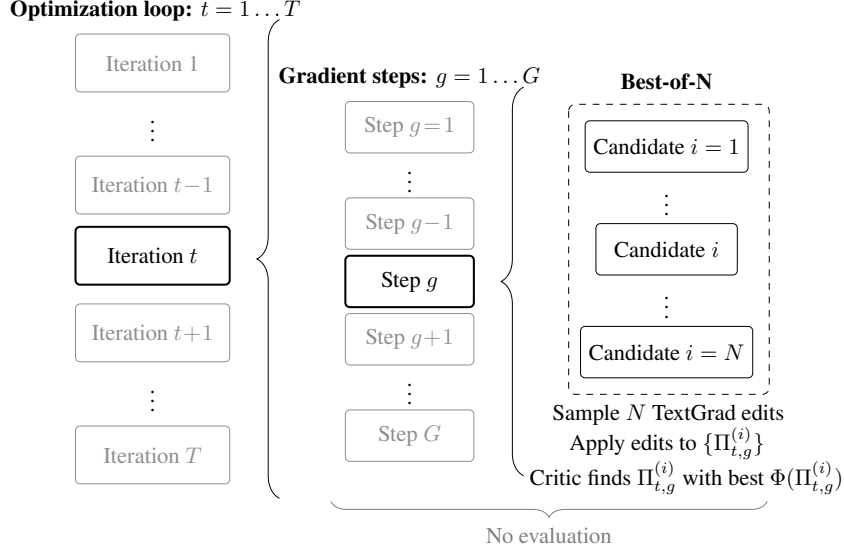


Figure 4: Summary of T-BoN BO: T iterations, G gradient steps, and Best-of- N candidates at each gradient step. T-BoN BO deliberately trades inexpensive generation compute for fewer evaluations: each iteration generates $N \times G$ prompt/outcome candidates with no evaluation.

- 1) **Textual gradient generation:** From the current inner prompt $\Pi_{t,g-1}$, query the textual-gradient generation operator $\nabla_{\text{text}}(\Pi_{t,g-1}; R_{t-1}, M_{\text{critic}})$ independently N times to obtain textual gradients $\{\delta_{t,g}^{(i)}\}_{i=1}^N$.
 - 2) **Candidate prompt generation:** Apply each textual gradient $\delta_{t,g}^{(i)}$ to $\Pi_{t,g-1}$ for all i to get $\{\Pi_{t,g}^{(i)}\}_{i=1}^N$.
 - 3) **Candidate system outcome generation:** Produce the system outcomes $\{c_{t,g}^{(i)} := \Phi(\Pi_{t,g}^{(i)})\}_{i=1}^N$.
 - 4) **Best-of- N selection:** Find the best of $\{(\Pi_{t,g}^{(i)}, c_{t,g}^{(i)})\}_{i=1}^N$ and set the best one as $(\Pi_{t,g}, c_{t,g})$.
2. **Evaluation.** (Detailed in Section 5.2) Set $c_t = c_{t,G}$ and $\Pi_t = \Pi_{t,g}$. Evaluate c_t to get the evaluation result s_t , i.e., $s_t = \text{Eval}(c_t, \mathcal{D}_{\mathcal{X}}(\Pi_t))$. Append (Π_t, c_t, s_t) to H_{t-1} to obtain H_t . If $s_t > s_{t-1}$, keep (Π_t, c_t) . Otherwise, set $(\Pi_t, c_t) = (\Pi_{t-1}, c_{t-1})$ and set $s_t = s_{t-1}$.⁶
 3. **Meta-reflection.** (Detailed in Section 5.3) Update the reflection $R_t \leftarrow \text{METAREFLECT}(H_t)$ for use at iteration $t+1$.

After T optimization steps, $\{c_t\}_{t=1}^T$ and $\{s_t\}_{t=1}^T$ are reported as the algorithm’s optimization outcome.

Note that T-BoN BO takes $N \times G$ generation of prompt/outcome candidates before one evaluation. This careful selection of a prompt/outcome candidate to evaluate is the key to evaluation efficiency in T-BoN BO: it deliberately trades inexpensive generation compute for fewer evaluations.

5.1 Best-of- N Textual Gradient steps.

At each gradient step $g = 1, \dots, G$, the algorithm expands the current prompt $\Pi_{t,g-1}$ into a neighborhood of N variants, then contracts back to a single survivor. The process begins with textual gradient generation: the

⁶This ‘gated’ acceptance/rollback was adopted from how Yuksekogul et al. [2025] implemented TEXTGRAD.

Algorithm 1: T-BoN BO

Input: System Φ ; initial prompt Π_0 ; critic M_{critic} ; candidates per step N ; gradient steps G ; iterations T

1 ; Output: Optimized Π_T, c_T, s_T

2 $c_0 \leftarrow \Phi(\Pi_0)$;

3 $s_0 \leftarrow \text{Eval}(c_0, \mathcal{D}_{\mathcal{X}}(\Pi_0))$;

4 $H_0 \leftarrow \{(\Pi_0, c_0, s_0)\}, R_0 \leftarrow \emptyset$;

5 **for** $t = 1$ **to** T **do**

6 $\Pi_{t,0} \leftarrow \Pi_{t-1}$;

7 **for** $g = 1$ **to** G **do**

8 **for** $i = 1$ **to** N **do**

9 $\delta_{t,g}^{(i)} \leftarrow$
 $\nabla_{\text{text}}(\Pi_{t,g-1}; R_{t-1}, M_{\text{critic}})$;

10 $\Pi_{t,g}^{(i)} \leftarrow \text{Apply}(\Pi_{t,g-1}, \delta_{t,g}^{(i)})$;

11 $c_{t,g}^{(i)} \leftarrow \Phi(\Pi_{t,g}^{(i)})$;

12 **end**

13 $(\Pi_{t,g}, c_{t,g}) \leftarrow$
 $\text{BEST-OF-N}(\{(\Pi_{t,g}^{(i)}, c_{t,g}^{(i)})\}, R_{t-1}, M_{\text{critic}})$

14 **end**

15 $c_t \leftarrow c_{t,G}, \Pi_t \leftarrow \Pi_{t,G}$;

16 $s_t \leftarrow \text{Eval}(c_t, \mathcal{D}_{\mathcal{X}}(\Pi_t))$;

17 $H_t \leftarrow H_{t-1} \cup \{(\Pi_t, c_t, s_t)\}$;

18 **if** $s_t < s_{t-1}$ **then**

19 $\Pi_t \leftarrow \Pi_{t-1}, c_t \leftarrow c_{t-1}, s_t \leftarrow s_{t-1}$;

20 **end**

21 $R_t \leftarrow \text{METAREFLECT}(H_t)$;

22 **end**

23 **return** $\{c_t\}_{t=1}^T$

Algorithm 2: Parallel T-BoN BO

Input: System Φ ; $\{\Pi_0^j\}_{j=1}^J$; critic M_{critic} ; candidates per step N ; gradient steps G ; iterations T ; J trajectories

Output: Optimized triples $\{(\Pi_T^j, c_T^j, s_T^j)\}_{j=1}^J$

1 **for** $j = 1$ **to** J **do**

2 $c_0^j \leftarrow \Phi(\Pi_0^j)$;

3 $s_0^j \leftarrow \text{Eval}(c_0^j, \mathcal{D}_{\mathcal{X}}(\Pi_0^j))$;

4 $H_0 \leftarrow \{(\Pi_0^j, c_0^j, s_0^j)\}, R \leftarrow \emptyset$;

5 **end**

6 **for** $t = 1$ **to** T **do**

7 **for** $j = 1$ **to** J **do**

8 $\Pi_{t,0}^j \leftarrow \Pi_{t-1}^j$;

9 **for** $g = 1$ **to** G **do**

10 **for** $i = 1$ **to** N **do**

11 $\delta_{t,g}^{j,(i)} \leftarrow$
 $\nabla_{\text{text}}(\Pi_{t,g-1}^j; R, M_{\text{critic}})$;

12 $\Pi_{t,g}^{j,(i)} \leftarrow$
 $\text{Apply}(\Pi_{t,g-1}^j, \delta_{t,g}^{j,(i)})$;

13 $c_{t,g}^{j,(i)} \leftarrow \Phi(\Pi_{t,g}^{j,(i)})$;

14 **end**

15 $(\Pi_{t,g}^j, c_{t,g}^j) \leftarrow$
 $\text{BEST-OF-N}(\{(\Pi_{t,g}^{j,(i)}, c_{t,g}^{j,(i)})\}, R_{t-1}, M_{\text{critic}})$

16 **end**

17 $c_t^j \leftarrow c_{t,G}^j, \Pi_t^j \leftarrow \Pi_{t,G}^j$;

18 $s_t^j \leftarrow \text{Eval}(c_t^j, \mathcal{D}_{\mathcal{X}}(\Pi_t^j))$;

19 $H_t \leftarrow H_{t-1} \cup \{(\Pi_t^j, c_t^j, s_t^j)\}$;

20 **if** $s_t^j < s_{t-1}^j$ **then**

21 $\Pi_t^j \leftarrow \Pi_{t-1}^j, c_t^j \leftarrow c_{t-1}^j$,

$s_t^j \leftarrow s_{t-1}^j$;

22 **end**

23 **end**

24 $R_t \leftarrow \text{METAREFLECT}(H_t)$;

25 **end**

26 **return** $\{c_t^{j*}\}_{t=1}^T$, where $j_t^* := \text{argmax}_j s_t^j$

Figure 5: T-BoN algorithm (Left) and Parallel T-BoN algorithm (Right).

critic model M_{critic} produces N improvement directions,

$$\delta_{t,g}^{(i)} \sim \nabla_{\text{text}}(\Pi_{t,g-1}; R_{t-1}, M_{\text{critic}}), \quad i = 1, \dots, N, \quad (5)$$

where randomness is introduced by a nonzero sampling temperature and nucleus filtering (top- p sampling)⁷, which ensures that the gradients are not identical but represent diverse, locally valid edits. Each textual gradient is then applied to form a candidate prompt

$$\Pi_{t,g}^{(i)} = \text{Apply}(\Pi_{t,g-1}, \delta_{t,g}^{(i)}), \quad (6)$$

with the rewrite operator configured for stability (low/zero temperature) so the edits remain coherent. The generator model then produces the system outcomes

$$c_{t,g}^{(i)} := \Phi(\Pi_{t,g}^{(i)}). \quad (7)$$

The system outcome candidates are reduced to one winner by the Best-of- N choice operation. For the Best-of- N choice operation, following Liu et al. [2025], we employ the pairwise tournament that uses critic model M_{critic} . First, the N candidates are permuted to produce randomly chosen tournament matches. Each match compares two outcomes $(c_{t,g}^{(i)}, c_{t,g}^{(j)})$ by querying M_{critic} for a head-to-head judgment (For the prompt, please refer to Figure 12 in Appendix A). illustrates the prompt example for ad generation tasks. To mitigate noise, the comparison is repeated K times (typically an even number to evenly swap orders to remove position bias [Shi et al., 2025], and break even by random; here we chose $K = 4$), producing votes $\{V_k(i, j)\}_{k=1}^K$, where $V_k(i, j) = i$ if critic prefers i over j , and vice versa. The winner of the pairwise match is then defined by the majority rule $\text{argmax}_{u \in \{i, j\}} \sum_{k=1}^K \mathbf{1}_{\{V_k(i, j) = u\}}$. Winners advance round by round until only one candidate remains. The survivor $(\Pi_{t,g}, c_{t,g}) = (\Pi_{t,g}^{(i^*)}, c_{t,g}^{(i^*)})$ is carried forward for the next gradient step $g + 1$.

5.2 Evaluation

After completing G gradient steps, we arrive at the $(\Pi_{t,G}, c_{t,G})$, which we redefine as (Π_t, c_t) . We evaluate (Π_t, c_t) : recall from Section 4 that (Π_t, c_t) is evaluated as

$$s_t := \frac{1}{L} \sum_{l=1}^L r\left(y\left(c_t, x_t^{(l)}\right)\right), \quad x_t^{(l)} \sim \mathcal{D}_{\mathcal{X}}(\Pi_t), \quad (8)$$

where $r\left(y\left(c_t, x_t^{(l)}\right)\right)$ is the evaluation of c_t for the input $x_t^{(l)}$ and L denotes the number of inputs evaluated. After evaluation, the triple (Π_t, c_t, s_t) is appended to the history H_{t-1} to form H_t . Following Yuksekgonul et al. [2025], we adopt a simple acceptance rule that controls progress: if $s_t \geq s_{t-1}$, the new candidate is adopted; otherwise, the system rolls back to the previous iteration’s outcome, i.e., $(\Pi_{t-1}, c_{t-1}, s_{t-1})$.

5.3 Meta-reflection.

At the end of each iteration t , we compress the full history H_t of prompts, generated system outcomes, and evaluation results into a natural language reflection R_t . R_t consists of a small set of actionable rules. In the ad

⁷In the experiments, we used Gemini Flash 2.5 with temperature = 0.8 and top $p = 0.9$.

generation example, those rules may take the form “emphasize social context,” “avoid cluttered backgrounds,” or “prefer warm lighting.” This reflection serves as a global memory; in subsequent iterations, the critic LLM takes this reflection as a part of its context when generating textual gradients. (For the prompt used for meta-reflection, see Figure 13 in Appendix A).

There are many ways to construct a reflection from past results. In our experiments, following Li et al. [2025b], we instruct the critic model M_{critic} to compare the five lowest- and five highest-performing outcomes from previous iterations (or, when fewer than ten are available, all outcomes)⁸, identify recurring visual and textual patterns, and distill them into a concise set of actionable rules.

5.4 Parallel T-BoN BO.

Although a local maximum found by gradient steps from a single starting point is often effective in practice, it may under-explore the ample prompt space. Following the practices [Wilson et al., 2018, Papenmeier et al., 2025], we also introduce a parallel variant of T-BoN BO that runs J optimization trajectories simultaneously (Algorithm 2). Here, each of J trajectories starts from a different initial prompt (denoted as $\{\Pi_0^j\}_{j=1}^J$). After independent gradient steps and evaluations at each iteration, evaluations from all trajectories are merged into the shared history, and a single meta-reflection is produced. Different trajectories diversify the search, while the shared reflection ensures that discoveries made by one trajectory are immediately shared with the others. Combined with the careful choice of gradients in T-BoN BO, this parallel process ensures the broader coverage of the search space and faster convergence to high-quality solutions in high-dimensional BO [Papenmeier et al., 2025] with a slight loss of optimality in the worst case [Wilson et al., 2018].

At the end of T optimization steps, the J -trajectory parallel T-BoN BO returns $\{(\Pi_T^j, c_T^j, s_T^j)\}_{j=1}^J$. For the purpose of reporting, for each $t \leq T$, we select $j_t^* := \operatorname{argmax}_j s_t^j$ and report its output $c_t^{j_t^*}$ as the step t ’s outcome. That is, $\{c_t^{j_t^*}\}_{t=1}^T$ is reported as the final outcome.

6 Theory: T-BoN BO’s Asymptotic Equivalence to UCB Bayesian Optimization

In this section, we prove that the Best-of- N over textual gradients selects, in probability, the ascent direction of the UCB acquisition with exploration weight β scaling as $\Theta(\sqrt{\ln N})$ (Theorem 2). What allows us to do rigorous theoretical analysis is that LLM prompt embeddings are invertible and bi-Lipschitz: LLM’s prompt embeddings are known to be injective, and therefore invertible [Nikolaou et al., 2025]; LLM embeddings are Lipschitz [Tang et al., 2025], implying they are bi-Lipschitz. Hence, small textual edits can be represented as small changes in the embedding space and vice versa. This enables us to map changes in prompts to changes in embeddings in Euclidean space, and later bring the theoretical guarantees back in the prompt space.

⁸Limiting the number of outcomes in the critic model’s context window helps mitigate context rotting [Hong et al., 2025].

Intuitive explanation.

Denote x to be an embedding of a prompt. Pick a small radius $\varepsilon > 0$ around x and sample N nearby edits $x_i = x + \varepsilon u_i$ with u_i on the unit sphere. Score each point

$$Y_i = \mu(x_i) + \xi_i \sigma(x_i), \quad \xi_i \text{ i.i.d. sub-Gaussian and independent of } \{u_i\}. \quad (9)$$

Let $M_N = \max_i \xi_i$ and $q_N = F^{-1}(1 - 1/N)$. Since $M_N \simeq q_N$ and $q_N = \Theta(\sqrt{\ln N})$, Best-of- N acts like picking the sampled x_i with the largest

$$\mu(x_i) + q_N \sigma(x_i). \quad (10)$$

On the small sphere around x the function $A_\beta(x') = \mu(x') + \beta \sigma(x')$ has a single best direction. Call it v_β . Draw a narrow cone around v_β . Then, with a large enough N , at least one u_i lands in that cone with high probability. The winner comes from that cone. Set $\beta = q_N$. Then Best-of- N behaves like UCB with weight β : it picks the sampled point most similar to the A_β best direction.

Rigorous derivation.

Let \mathcal{M} be the set of syntactically valid prompts. Suppose that there exists a text embedding $E : \mathcal{M} \rightarrow \mathbb{R}^d$, where $x := E(\Pi) \in \mathbb{R}^d$ is the embedding of a prompt $\Pi \in \mathcal{M}$. We first state the assumptions motivated by how language model embeddings behave in practice, and then state the main theorem, Theorem 2.

At each gradient step of T-BoN BO, we sample edits that correspond to $u_1, \dots, u_N \stackrel{\text{i.i.d.}}{\sim} \rho$ on the embedding space $\subset \mathbb{R}^d$, where ρ is assumed to have a density bounded below by a positive constant with respect to surface measure. Assumption 1 implies that small textual edits induce near-linear moves in \mathbb{R}^d , consistent with the recent findings that prompt embeddings preserve phrase similarity under small changes [Reimers and Gurevych, 2019, He et al., 2025, Tang et al., 2025, Nikolaou et al., 2025].

Assumption 1 (Embedding map and edit realization). *For the current prompt Π with $x = E(\Pi)$, constants $C < \infty$ and $\varepsilon_0 > 0$ such that for every unit vector $u \in \mathbb{R}^d$ and every $\varepsilon \in (0, \varepsilon_0]$ the edit operator Apply realizes a first-order move:*

$$E(\text{Apply}(\Pi, \varepsilon u)) = x + \varepsilon u + r(\varepsilon, u), \quad \sup_{\|u\|=1} \|r(\varepsilon, u)\| \leq C \varepsilon^2. \quad (11)$$

Next, the assumption 2 is a standard regularity/technical condition: let's call a function $f : \mathbb{R}^d \rightarrow \mathbb{R}$ is $C^{1,1}$ if it is continuously differentiable and its gradient is Lipschitz: $\exists L < \infty$ such that $\|\nabla f(y) - \nabla f(z)\| \leq L\|y - z\|$ for all y, z .

Assumption 2 (μ, σ are of $C^{1,1}$). *Let $\mu(x)$ and $\sigma(x)$ denote the mean and standard deviation of the evaluation variable Y at embedding x . We assume μ, σ are $C^{1,1}$ locally. We use $g = \nabla \mu(x)$ and $h = \nabla \sigma(x)$.*

Assumption 3 specifies a heteroscedastic sub-Gaussian model for candidate scores (with i.i.d. mean-zero,

unit-variance, unbounded-support noise independent of the sampled directions) and an ideal Best-of- N choice oracle.

Assumption 3 (Noise model and choice oracle). *Let $\{\xi_i\}_{i=1}^N$ be i.i.d. mean-zero, unit-variance, Gaussian random variables with unbounded support, independent of $\{u_i\}$. For candidates $x_i := x + \varepsilon u_i$ we observe*

$$Y_i = \mu(x_i) + \sigma(x_i) \xi_i, \quad (12)$$

and the Best-of- N oracle returns $i^* \in \arg \max_{i \in [N]} Y_i$.

Assumption 4 (Small-step regime and limit order). *We take limits with $N \rightarrow \infty$ first, then $\varepsilon \downarrow 0$.*

Lemma 1 (Gaussian maxima and spacing [Vershynin, 2018]). *Let ξ_1, \dots, ξ_N be i.i.d. mean-zero, unit-variance Gaussian, $M_N = \max_{i \leq N} \xi_i$, S_N the second largest, and $q_N := F^{-1}(1 - 1/N)$ the $(1 - 1/N)$ -quantile of ξ_1 . Then $q_N = \Theta(\sqrt{\ln N})$, $M_N - q_N \rightarrow 0$ in probability, and $M_N - S_N = O_p(1/q_N)$.*

Theorem 2 (Best-of- N asymptotically induces a UCB gradient direction). *Under Assumptions 1-4, define $\beta_N := q_N$ from Lemma 1. Let $i^* \in \arg \max_i Y_i$ and set $\hat{u}_N := u_{i^*}$. Define the step*

$$\Delta x^{(N)} := \mathbb{E}(\text{Apply}(\Pi, \varepsilon \hat{u}_N)) - x = \varepsilon \hat{u}_N + r(\varepsilon, \hat{u}_N). \quad (13)$$

Then, with the limit order $N \rightarrow \infty$ first and $\varepsilon \downarrow 0$ second,

$$\frac{\Delta x^{(N)}}{\|\Delta x^{(N)}\|} = \hat{u}_N \xrightarrow{p} \frac{\nabla A_{\beta_N}(x)}{\|\nabla A_{\beta_N}(x)\|} = \frac{g + \beta_N h}{\|g + \beta_N h\|}. \quad (14)$$

Moreover,

$$A_{\beta_N}(x + \Delta x^{(N)}) \geq A_{\beta_N}(x) + \varepsilon \|\nabla A_{\beta_N}(x)\| - o_p(\varepsilon). \quad (15)$$

7 Case Study: Ad Optimization in Digital Marketing

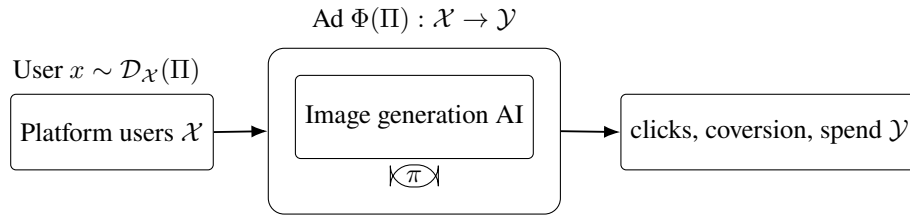


Figure 6: An ad generation AI system Φ and prompt $\Pi = \langle \pi \rangle$.

In this section, we present a case study on how ad platforms can use T-BoN BO for ad optimization and automate the ad generation, analysis, and evaluation cycle. Given an a priori fine-tuned image generation AI model that is aligned with its client’s brand, the objective is to efficiently refine the prompts for ad generation to better align with the users’ preference distribution.

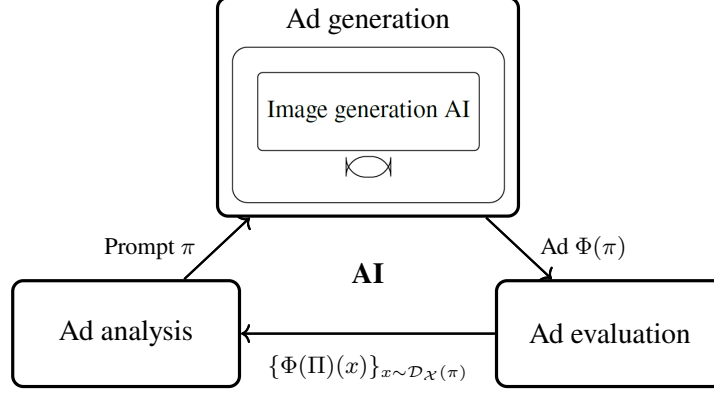


Figure 7: A self-improving AI implemented on the ad generation AI system in Figure 6.

7.1 Problem definition

Formally, define the brand fine-tuned ad-generation AI system as Φ , whose behavior is controlled by a prompt set Π (Figure 6). For a given prompt set Π , we write $\Phi(\Pi)$ for the corresponding ad creative shown on the ad platform. As a system, $\Phi(\Pi)$ maps the input space \mathcal{X} (potential ad viewers on the platform) to a distribution over the output space \mathcal{Y} (observable ad responses). For each $x \in \mathcal{X}$, we denote by $y(\Phi(\Pi), x)$ the random \mathcal{Y} -valued output of the system at input x . In a digital marketing setting, x is a platform user, and a realization of $y(\Phi(\Pi), x)$ represents that user’s reaction (e.g., clicks, conversions, spend) to the ad $\Phi(\Pi)$. When a user $x \in \mathcal{X}$ is shown the ad creative $\Phi(\Pi)$, we observe an outcome $y \in \mathcal{Y}$, which is a realization of $y(\Phi(\Pi), x)$.

As discussed earlier, the distribution of exposed users depends on the ad $\Phi(\Pi)$ and therefore on the prompt set Π . We denote by $\mathcal{D}_{\mathcal{X}}(\Pi)$ the unknown distribution of users x who are shown the ad generated from Π when the ad $\Phi(\Pi)$ is run on the platform.

To evaluate system performance, a marketer pre-defines a scoring rule $r : \mathcal{Y} \rightarrow [0, 1]$ that maps observed user responses (clicks, conversions, spend) to a normalized effectiveness score. The ad optimization objective of the agency for a given client and campaign can then be written as

$$J(\Pi) := \mathbb{E}[r(y(\Phi(\Pi), x))], \quad (16)$$

where the expectation is taken over $x \sim \mathcal{D}_{\mathcal{X}}(\Pi)$ and any additional randomness in $y(\Phi(\Pi), x)$.

The self-improving ad system built by the agency can therefore be viewed as an iterative algorithm that searches over prompts π in order to maximize $J(\pi)$ while minimizing the number of costly ad evaluations on the platform (Figure 7). At iteration t , a candidate prompt π_t is selected, the corresponding ad creative $\Phi(\pi_t)$ is generated, and the campaign is (conceptually) exposed to a batch of users $\{x_t^{(l)}\}_{l=1}^L \sim \mathcal{D}_{\mathcal{X}}(\pi_t)$. The empirical evaluation

$$s_t := \frac{1}{L} \sum_{l=1}^L r(y(\Phi(\pi_t), x_t^{(l)})) \quad (17)$$

serves as a noisy estimate of $J(\pi_t)$ and is fed back into the optimization algorithm (T-BoN BO) to update the history H_t and the meta-reflection R_t .

7.2 Application of T-BoN BO

We now describe how the general T-BoN BO framework in Section 5 is instantiated for ad agency’s ad optimization problem. Specifically, we focus on the parallel version of T-BoN BO (Algorithm 2), where J optimization trajectories start from different initial prompts and run simultaneously.

Initialization. The decision-maker/platform starts from initial prompts $\{\pi_0^j\}_{j=1}^J$, i.e., prompts already in use or high-quality baselines provided by humans. (e.g., “A simple, photorealistic image of a plant-based burger patty.”⁹) For each initial prompt π_0^j , the system generates an ad $\Phi(\pi_0^j)$ and obtains an initial score s_0^j by deploying the ad and observing outcomes. These tuples $\{(\pi_0^j, \Phi(\pi_0^j), s_0^j)\}_{j=1}^J$ form the initial history H_0 for the parallel T-BoN BO procedure.

Best-of- N textual-gradient steps. Within each optimization iteration t , T-BoN BO refines each trajectory’s prompt π_{t-1}^j through G Best-of- N textual-gradient steps (Figure 4). For a given trajectory j and inner step g , the critic model M_{critic} (a large language model such as Gemini 2.5 Flash) receives as context: (i) the current prompt $\pi_{t,g-1}^j$, (ii) the current meta-reflection R_{t-1} , and (iii) a short description of the brand and campaign scenario. Conditioned on this context, it proposes N small natural-language edits

$$\delta_{t,g}^{j,(1)}, \dots, \delta_{t,g}^{j,(N)} \sim \nabla_{\text{text}}(\pi_{t,g-1}^j; R_{t-1}, M_{\text{critic}}), \quad (18)$$

which form the textual gradients. Each edit is then applied to the current prompt to obtain N candidate prompts

$$\pi_{t,g}^{j,(i)} \leftarrow \text{Apply}(\pi_{t,g-1}^j, \delta_{t,g}^{j,(i)}), \quad i = 1, \dots, N. \quad (19)$$

These textual gradients correspond to small, directed moves in language space that, according to the critic’s judgment, are likely to increase ad effectiveness. For example, conditioned on the reflection R_{t-1} (e.g., “social occasions and visible grill marks tend to perform better than plain pack shots”), the critic M_{critic} may propose the following textual-gradient candidates:

1. *Emphasize social context and enjoyment:* “Show the burger being enjoyed at an outdoor barbecue with friends, not alone on a plate.”
2. *Highlight sensory appeal and indulgence:* “Make the patty look extra juicy with clear grill marks, a toasted bun, and melty toppings.”
3. *Make sustainability salient but secondary:* “Subtly include eco-friendly cues (like a small ‘plant-based’ tag or greenery in the background) without overpowering the food.”

⁹Note that in the experiments in Section 8, we use WORST5-OF-N prompts as initial starting points, which are higher-quality, much more detailed initial prompts; See Appendix A.

Each of these textual gradients $\delta^{(i)}$ is then applied to the original prompt to produce candidate prompts. For example, applying the first gradient yields the prompt:

“A photorealistic image of a juicy plant-based burger with grill marks, served at a vibrant summer barbecue with friends, everyone smiling and reaching for food.”

Applying the second gradient yields the prompt:

“A close-up, photorealistic shot of a plant-based burger with deep grill marks, a toasted brioche bun, melty vegan cheese, fresh toppings, and steam rising to suggest warmth and juiciness.”

To select the next prompt that will go forward to the next gradient step among N candidate prompts $\{\pi_{t,g}^{j,(i)}\}_{i=1}^N$, T-BoN BO applies the Best-of- N choice rule over the N corresponding candidate ads $\{c_{t,g}^{j,(i)}\}_{i=1}^N$. Following Liu et al. [2025], we implement Best-of- N via a pairwise tournament: in each match, the critic model M_{critic} compares two creatives side by side and predicts which will perform better, given the campaign goals and the current meta-reflection R_{t-1} (see Figure 12 in Appendix A). After multiple randomized pairwise comparisons, the winner $c_{t,g}^j$ and its corresponding prompt $\pi_{t,g}^j$ are carried forward to the next gradient step. Repeating this expansion-and-selection process for $g = 1, \dots, G$ yields the refined prompt π_t^j and ad $\Phi(\pi_t^j)$ for trajectory j at iteration t .

Evaluation as the costly step. Once all G gradient steps are completed, T-BoN BO performs a single expensive evaluation for each trajectory by deploying the ad $\Phi(\pi_t^j)$ and computing the score s_t^j . In the real ad-agency use case, this evaluation step would correspond to running the creative in an A/B test, multi-armed bandit experiment, or survey-based study, and mapping the resulting performance metrics to a scalar score via the scoring rule r . The new triple $(\pi_t^j, \Phi(\pi_t^j), s_t^j)$ is appended to the history H_t , and a simple acceptance rule is applied: if s_t^j fails to improve upon s_{t-1}^j , the trajectory rolls back to $(\pi_{t-1}^j, \Phi(\pi_{t-1}^j), s_{t-1}^j)$.

Meta-reflection shared across trajectories. After all J trajectories have been evaluated at iteration t , the algorithm updates the global meta-reflection $R_t = \text{METAREFLECT}(H_t)$, as in Section 5.3. Concretely, M_{critic} is prompted to review a subset of the best- and worst-performing ads and prompts in H_t and to summarize the key patterns and rules that distinguish successful creatives from unsuccessful ones (see Figure 13 in Appendix A). For example, the reflection may emphasize that scenes with social eating and visible grill marks perform better than isolated product shots, or that emphasizing “satisfying” and “juicy” yields higher effectiveness scores. This reflection is then injected into the context of subsequent textual-gradient generation and Best-of- N comparisons, allowing all trajectories to share accumulated knowledge even though they explore different regions of the prompt space.

Reported outcome. After T iterations, the system returns the sequence of best-performing ads $\{c_t^{j^*}\}_{t=1}^T$, where $j_t^* = \arg \max_j s_t^j$ is the trajectory that achieves the highest score at iteration t .

8 Experiments

We validate the empirical effectiveness of the proposed T-BoN BO framework for a real-world digital marketing problem described in 7. Specifically, we examine if and how much T-BoN BO improves outcomes under a fixed evaluation budget compared to state-of-the-art baselines.

8.1 Evaluation Module using Persona data and LLM-based Simulation

To evaluate how well an ad performs on the target population and improve prompts, we need a target population and a way to measure the preferences of that population for a given ad. There are many ways to do this, such as field experiments, consumer surveys, or simulated responses from a pre-defined target population. In our experiments, we use LLM-generated preferences over the Twin-2k-500 persona distribution provided by Toubia et al. [2025]. An important advantage of using this persona distribution is that it allows us to test the performance of different algorithms fast without the need for large-scale field experiments or expensive surveys.¹⁰

This dataset includes the data of 2,058 U.S. adults answering 500 survey questions spanning demographics, personality, cognitive ability, economic preferences, classic heuristics-and-biases tasks, and a pricing study. These survey questions of each persona are passed to a multi-modal LLM (Gemini 2.5 Flash) as context so that the LLM can simulate the ad effectiveness for the persona.¹¹ We divided the Twin-2k-500 personas into 80% (1647 personas) for the training set and 20% (411 personas) for the test set. Every time we evaluate an ad during the algorithm (i.e., training stage), we randomly sample 200 personas from the training set and simulate the ad’s effectiveness for them. Every time we want to test an ad, such as a final ad output from the algorithm, we simulate its effectiveness for all the test set personas.

8.2 Experiment Setup

We consider eight synthetic ad campaign scenarios that cover a diverse range of products across distinct categories, defined by the creative brief that outlines the strategic and creative direction for each scenario. (For the creative brief for each scenario, see Appendix B.)

- Scenario 1: “GreenBite,” a new plant-based burger patty.
- Scenario 2: “AuraSonics X1,” high-end, noise-canceling wireless earbuds.
- Scenario 3: “Odyssey E-SUV,” a new all-electric family SUV.
- Scenario 4: “Oasis Eco-Lodge,” a secluded, luxury resort with beautiful natural surroundings.
- Scenario 5: “Momentum,” a mobile-first banking app for freelancers and the gig economy.
- Scenario 6: “MindGarden,” a subscription-based meditation and mindfulness app.

¹⁰Note that naive field deployment cannot be used to test the relative performance of algorithms since an algorithm’s measured advantage would be a mix of its own effect and distributional effects induced by the ad platform’s ad targeting systems.

¹¹While LLM-based persona simulation is often biased and does not reflect real-world human behavior [Li et al., 2025a, Peng et al., 2025], it still induces a valid preference distribution for which, as a benchmark, we would like to see how well a method can optimize.

- Scenario 7: “Aeterno,” a classic, automatic Swiss-made wristwatch with a heritage design.
- Scenario 8: “SyncFlow,” a project management and collaboration software platform for remote teams.

For each scenario, from its creative brief, we generated 64 high-quality initial prompts that were used as input to the state-of-the-art image generation AI model named Imagen 4¹² to generate the initial 64 high-quality ads. (For prompts, see Figure 14 and 15 in Appendix A.) To maintain a rigorous baseline, we made the 64 initial prompts detailed enough to yield strong ads. This ensures that the algorithm’s subsequent improvements are not explained as trivial quality gains from having initial under-specified prompts. That is, the measured improvements are attributed to the algorithm’s ability to align ads with the underlying persona distribution better.

When simulating an ad’s effectiveness for a persona, we ask the LLM (with the prompt in Figure 8) what the ad’s “effectiveness”¹³ for the persona will be, with the score of [1, 2, 3, 4, 5]. Here, the score of one is the least effective, and the score of five is the most effective. As the LLM’s internal assignment of probability for the scores is available as ‘logprobs’¹⁴, we use them to calculate the mean score, and consider it as the evaluation score of the ad for the persona (which is a fraction number like 3.41), instead of considering the actual response score from the LLM (which is an integer number among 1-5). We then take the average of the evaluation scores for the personas to get the final evaluation score of the ad.

```

Persona prompt for simulating ad effectiveness.

PERSONA DATA: {
Which part of the United States do you currently live in? [Answer]
What is the highest level of schooling or degree that you have completed? [Answer]
... (Many other survey questions and answers) ...
Suppose you were given 5 and had to offer to another (anonymous) person a way to split the money... [Answer]
... (Many other survey questions and answers) ...
}

AD IMAGE: [image]

TASK: Return only one item from ["1","2","3","4","5"] for ad effectiveness.
Effective Score Scale Definition:
1: Extremely Unlikely. The persona would actively ignore or be annoyed by this ad.
2: Unlikely. The persona would likely scroll past without a second thought.
3: Mediocre. It is hard to decide whether the personal would click or don't click.
4: Likely. The persona is intrigued and has a good chance of clicking to learn more.
5: Extremely Likely. The persona is the ideal target; a click is almost certain.
No explanation. Just the score.

```

Figure 8: Persona simulation prompt for the digital marketing problem.

Among the initial ads, we identified the best initial ad, which we call BEST-OF-64, and the worst five initial

¹²See Vertex AI’s description (<https://console.cloud.google.com/vertex-ai/publishers/google/model-garden/imagen-4.0-generate-preview-06-06>) for details.

¹³The vagueness of the term “effectiveness” constitutes an evaluation distribution induced by LLM-persona based on what LLM ‘thinks’ about the term, which we target to align the algorithms with. That is, as long as we consistently query the same LLM to predict “effectiveness” using the same prompt, such vagueness is justified.

¹⁴See Vertex AI’s logprobs description (<https://cloud.google.com/vertex-ai/generative-ai/docs/model-reference/inference#logprobs>) for details.

ads, which we call WORST5-OF-64, by running a best-arm identification bandit algorithm [Russo, 2016] by alternating the best-arm identification objective and worst 5-arm identification objective for evaluations of 5,000 sequential random samples from the training persona set.

8.3 Baselines

As baselines, we consider the performance of two popular state-of-the-art algorithms. One is the BEST-OF-64 [Snell et al., 2024] baseline, which is one of the most popular and well-performing test-time alignment methods that has been reported to outperform reinforcement learning fine-tuning methods under large enough N [Gao et al., 2023, Mudgal et al., 2023, Eisenstein et al., 2023, Beirami et al., 2024]. Specifically, the test persona set-based evaluation result for the Best-of-64 ad (identified above in Section 8.2 using training persona set) was used as the BEST-OF-64 baseline. We also evaluated the ads in Worst5-of-64 in the same way and took the mean of their scores to obtain the WORST5-OF-64 baseline.

Another baseline is GEPA (Genetic-Pareto) [Agrawal et al., 2025]. As discussed earlier, this reflective and evolutionary prompt evolution algorithm has recently demonstrated superior performance compared to GRPO [Liu et al., 2024a], a state-of-the-art reinforcement fine-tuning technique. GEPA keeps a set of candidate prompts, and samples a prompt to mutate based on its evaluation result for a problem (in our case, a persona) set they call the Pareto set. A Pareto set stores ‘important’ problems. Since we randomly sample personas from the training persona set, we cannot store specific personas and retrieve them later. Therefore, we instead use the version of GEPA that 1) randomly samples a persona and 2) mutates all candidate prompts equally and throws away the old prompts to avoid unbounded growth of the candidate set.

For the experiment, we run five-trajectory ($J = 5$) parallel T-BoN BO and GEPA starting from Worst5-of-64, i.e., the worst five initial prompts we identified in Section 8.2. This starting point allows us to attribute observed gains to the algorithms rather than to favorable starting prompts. We test if T-BoN BO outperforms the BEST-OF-N baseline and GEPA baseline throughout the optimization process. For both T-BoN BO and GEPA, we ran 10 optimization steps, evaluating 200 randomly sampled personas per step (2,000 total persona evaluations). We used a multi-modal LLM (Gemini-2.5-Flash) to serve as the critic model for both T-BoN BO and GEPA.

8.4 Results and Analysis

Trend analysis

Figure 9 plots how much T-BoN BO, GEPA, and BEST-OF-N improved their performance from the initial WORST5-OF-N score across eight scenarios. (For the detailed data used to generate this plot, refer to Table 2 and 3 in Appendix C.) At each step (the x -axis), the performance score (the y -axis) is the average of eight scenarios’ mean evaluation score for the testing persona set. For example, the step-2 score is the average of the eight step-2 mean evaluation scores. As the figure illustrates, both T-BoN BO and GEPA improve consistently across steps, with T-BoN BO demonstrating faster early gains and achieving a significantly better final performance than GEPA. Notably, by the third step on average, which is equivalent to 600 persona evaluations, T-BoN BO and GEPA both outperform the BEST-OF-64 baseline.

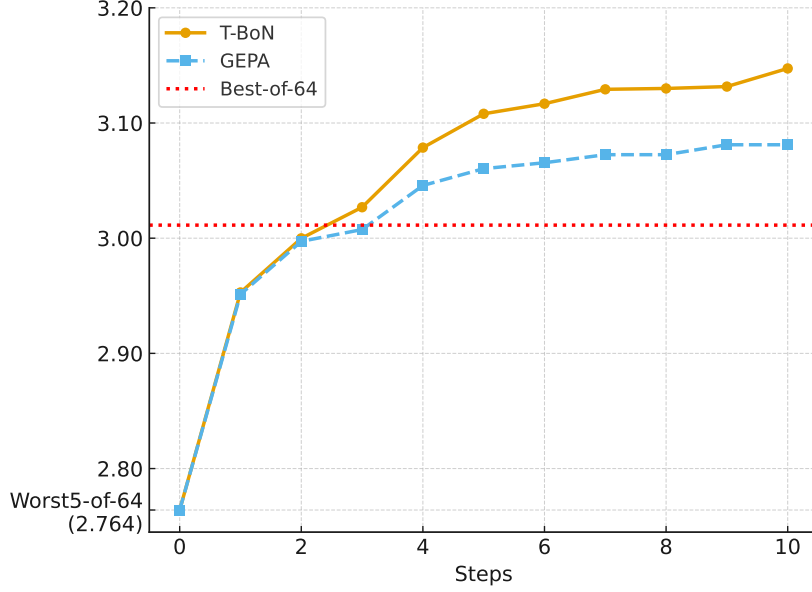


Figure 9: Progress comparison of T-BoN BO and GEPA with BEST-OF-64 baseline. T-BoN BO implements parallel T-BoN BO with $J = 5$. The performance score (the y -axis) is the average of eight scenarios’ mean evaluation score for the testing persona set. Since it is the mean of means, we don’t plot the standard errors.

Statistical analysis

<i>Model</i>			
score = $\alpha + \beta_1 \mathbf{1}\{t = 10\} + \beta_2 \mathbf{1}\{\text{TBoN}\} \mathbf{1}\{t = 10\} + \text{persona FE} + \text{scenario FE} + \varepsilon$			
<i>Effect</i>	Estimate	Std. err	T-stat
β_1 : GEPA gain ($t = 10$) from WORST5-OF-64	0.3168***	0.0325	9.752
β_2 : T-BoN BO gain - GEPA gain ($t = 10$) from WORST5-OF-64	0.0743***	0.0248	2.991
$\beta_1 + \beta_2$: T-BoN BO gain ($t = 10$) from WORST5-OF-64	0.3911***	0.0355	11.011
<i>Summary statistics</i>			
Observations		13,152	
Personas		411	
Scenarios		8	

Notes: Two-way cluster-robust standard errors. * $p < 0.10$, ** $p < 0.05$, *** $p < 0.01$.

Table 1: Two-way fixed effect (TWFE) analysis result with persona and scenario fixed effects with two-way clustered SEs [Cameron et al., 2011]. Standard error of $\beta_1 + \beta_2$ was computed using Delta method.

In addition to the aggregate trend analysis provided in Figure 9, we now provide statistical evidence that T-BoN BO indeed outperforms the GEPA. For this, we conducted a Two-way Fixed Effect (TWFE) analysis using T-BoN BO and GEPA’s final ($t = 10$) scores to compare the effectiveness of each method rigorously.

Specifically, we consider the following TWFE model:

$$\text{score} = \alpha + \beta_1 \mathbf{1}\{t = 10\} + \beta_2 \mathbf{1}\{\text{TBoN}\} \mathbf{1}\{t = 10\} + \text{persona FE} + \text{scenario FE} + \varepsilon. \quad (20)$$

where $\mathbf{1}\{t = 10\}$ is the indicator variable of whether it is $t = 0$ (GEPA and T-BoN BO’s initial starting point, i.e., WORST5-OF-64 score) or $t = 10$ (GEPA and T-BoN BO’s final score), β_1 is the GEPA’s gain from WORST5-OF-64 after $t = 10$, β_2 is the T-BoN BO’s advantage over GEPA after $t = 10$, and $\beta_1 + \beta_2$ is the T-BoN BO’s gain from WORST5-OF-64 after $t = 10$. The unobserved residual ε is assumed to follow the normal distribution. To remove potential correlation among unobserved residuals within the same persona or scenario, we conducted a cluster-robust Two-way Fixed Effect (TWFE) analysis with two-way clustering [Cameron et al., 2011, Cameron and Miller, 2015]. The result of TWFE analysis is shown in Table 1. As we can see, both of T-BoN BO’s gain and GEPA’s gain from the starting point (WORST5-OF-64) after $T = 10$ are statistically significant. In addition, we conclude that T-BoN BO has a significant 23.5% more gain in score compared to GEPA’s gain.

Qualitative analysis

The significant gains of GEPA and T-BoN BO can be interpreted as demonstrating their ability to align with the persona distribution. However, such significance can also be easily gained by starting from a poor starting point, i.e., a poor WORST5-OF-N prompt and corresponding ad image. One way to check whether this happens is to compare the quality of the prompts; we provide them in Appendix A to demonstrate that this is not the case. Another qualitative approach is to compare the generated ad images and verify whether the differences among ads are in quality or in the message and representation. Figure 10 compares the ad images of the baseline methods. As we can see, there is no clear visual quality difference among those ad images; the differences are mainly in the ad’s message and how it is represented. This supports the claim that T-BoN BO and GEPA improvements from WORST5-OF-N demonstrated in Figure 9 are attributed to alignment, not trivial quality gains from correcting poor or under-specified prompts.

8.5 Ablation study

The main experiment in Section 8.1-8.4 evaluates the candidate ad at each iteration as the mean of scores across 411 personas (20% of the persona data in Twin-2k-500 [Toubia et al., 2025]) that were injected into the LLM’s context. Each persona consists of a large amount of information, with 500 survey questions accounting for around 50,000 tokens. Would T-BoN BO still outperform strong state-of-the-art baselines when the LLM receives less persona context information?

To test this, we ran a no-persona ablation experiment in which the evaluator is a single LLM (Gemini 2.5 Flash) with no auxiliary persona context. Concretely, at each iteration, we present only the ad image candidate to LLM judge (Gemini 2.5 Flash) together with the same 1–5 effectiveness rubric, set temperature to 0, and compute the same scalar score as the log-probability-weighted expectation over $\{1, \dots, 5\}$ as before.¹⁵ This

¹⁵With temperature = 0, the judge’s output is deterministic for a fixed image and rubric; the logprob vector is still available, so the expected score is stable across repeated calls.

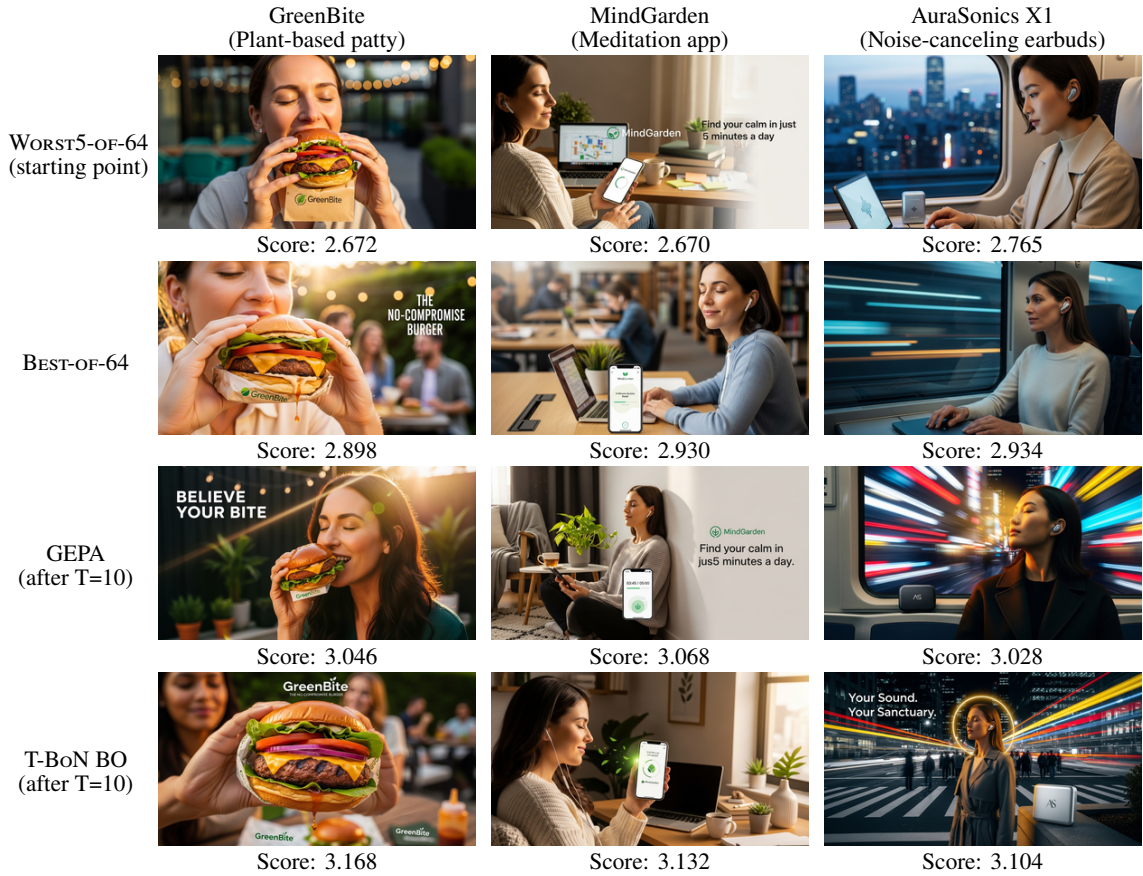


Figure 10: T-BoN BO and baseline’s generated Ad images for three fictional brands: GreenBite burger patty (Scenario 1), MindGarden meditation app (Scenario 6), and AuraSonics noise-canceling earbuds (Scenario 2). For the Ad images of the other five brand scenarios, see Figure 18 in Appendix C.

collapses the evaluation to a deterministic mapping and removes heterogeneity from personas and sampling, allowing us to test whether T-BoN BO’s performance depends on specific persona information-related setup. To ensure there is no leakage of preference, we used GPT-5 instead of Gemini 2.5 Flash for generating meta-reflection, generating textual gradients, and making Best-of-N choices.

We again compare T-BoN BO ($J=5$ trajectories) against the BEST-OF-64 initial baseline; we exclude GEPA, which requires multiple personas (multiple problems, in GEPA’s language.)

Figure 11 plots T-BoN BO across 10 optimization steps starting from the WORST5-OF-64 prompts under the ablation setup. As in Figure 9, the main experiment’s results, the value shown in Figure 11 is the mean of that step’s scores over eight scenarios. As can see in Figure 11, T-BoN BO again outperforms BEST-OF-64 baseline from optimization step 3. Except for the fact that in general the evaluation scores without persona information are more optimistic than scores with persona information for both T-BoN BO and BEST-OF-64, the ablation experiment’s trend in Figure 11 shows the same trend we saw in Figure 9.

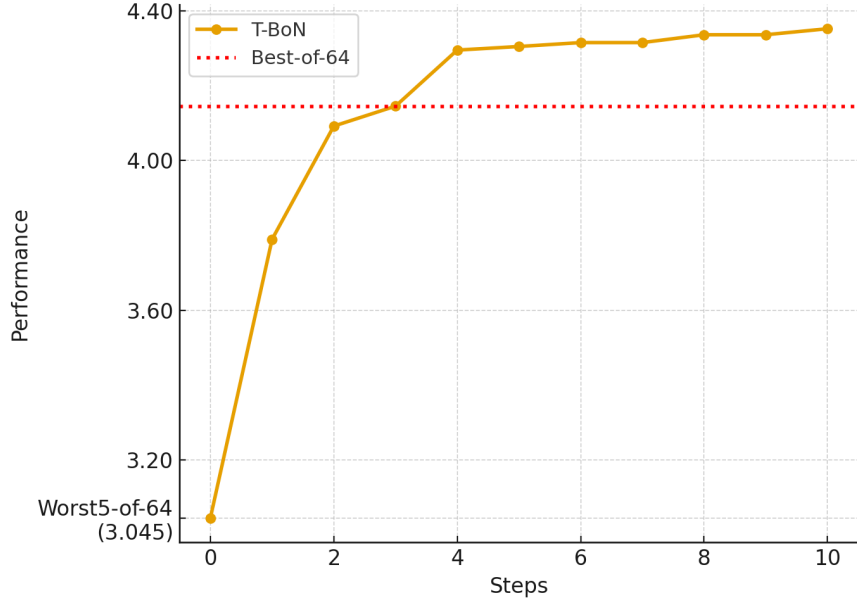


Figure 11: An ablation study experimenting T-BoN BO with $J = 5$ and BEST-OF-64 for Gemini 2.5 Flash instead of persona distribution with temperature 0. (GEPA was excluded, as there is no problem-dependent heterogeneity.) The performance score (the y -axis) is the average of eight scenarios’ mean evaluation score for the testing persona set. Again, since it is the mean of means, we don’t plot the standard deviations.

9 Conclusion

The importance of developing evaluation-efficient self-improving AI systems is substantial for its societal applications, yet this problem has remained unidentified and unaddressed. Motivated by the effectiveness of prompt optimization, which outperforms reinforcement fine-tuning methods, we formulate this problem as an iterative prompt optimization and address it.

We propose T-BoN BO, a simple, evaluation-efficient prompt optimization framework that leverages textual edits and Best-of- N search to guide prompt improvement. We prove that T-BoN BO BO statistically emulates UCB-BO, which is a provably evaluation-efficient algorithm. Experiments simulating ad alignment across eight creative-ad tasks demonstrate that T-BoN BO outperforms strong state-of-the-art baselines, including large BEST-OF- N and GEPA. We validate that these improvements are not attributed to the usage of specific persona dataset or trivial improvements from using poor initial prompts.

Our paper makes three key contributions to the computer science and marketing literature. First, it identifies evaluation efficiency as an essential objective for a societal self-improving system design. Second, it presents a simple yet provably efficient AI self-improving system design framework that can be applied to real-world societal systems, e.g., ad agencies, that incur high evaluation costs. Third, we theoretically prove that the presented framework is evaluation-efficient.

In sum, this work bridges classical Bayesian optimization and prompt-based self-improving AI systems, demonstrating that evaluation-efficient optimization in the prompt space is both theoretically tractable and

practically impactful. As organizations increasingly rely on AI-generated content, methods like T-BoN BO can help managers achieve higher-quality outputs without proportionally increasing evaluation burdens.

References

- Emre Can Acikgoz, Cheng Qian, Heng Ji, Dilek Hakkani-Tür, and Gokhan Tur. Self-improving llm agents at test-time. *arXiv preprint arXiv:2510.07841*, 2025.
- Virginia Aglietti, Ira Ktena, Jessica Schrouff, Eleni Sgouritsa, Francisco Ruiz, Alan Malek, Alexis Bellot, and Silvia Chiappa. Funbo: Discovering acquisition functions for bayesian optimization with funsearch. In *Forty-second International Conference on Machine Learning*, 2025.
- Lakshya A Agrawal, Shangyin Tan, Dilara Soylu, Noah Ziemis, Rishi Khare, Krista Opsahl-Ong, Arnab Singhvi, Herumb Shandilya, Michael J Ryan, Meng Jiang, et al. Gepa: Reflective prompt evolution can outperform reinforcement learning. *arXiv preprint arXiv:2507.19457*, 2025.
- Nicolás Aramayo, Mario Schiappacasse, and Marcel Goic. A multiarmed bandit approach for house ads recommendations. *Marketing Science*, 42(2):271–292, 2023.
- Wenjia Ba, J Michael Harrison, and Harikesh S Nair. Advertising media and target audience optimization via high-dimensional bandits. *arXiv preprint arXiv:2209.08403*, 2022.
- Ahmad Beirami, Alekh Agarwal, Jonathan Berant, Alexander D’Amour, Jacob Eisenstein, Chirag Nagpal, and Ananda Theertha Suresh. Theoretical guarantees on the best-of-n alignment policy. *arXiv preprint arXiv:2401.01879*, 2024.
- Nitay Calderon, Roi Reichart, and Rotem Dror. The alternative annotator test for llm-as-a-judge: How to statistically justify replacing human annotators with llms. *arXiv preprint arXiv:2501.10970*, 2025.
- A Colin Cameron and Douglas L Miller. A practitioner’s guide to cluster-robust inference. *Journal of human resources*, 50(2):317–372, 2015.
- A Colin Cameron, Jonah B Gelbach, and Douglas L Miller. Robust inference with multiway clustering. *Journal of Business & Economic Statistics*, 29(2):238–249, 2011.
- Kaiyuan Chen, Yixin Ren, Yang Liu, Xiaobo Hu, Haotong Tian, Tianbao Xie, Fangfu Liu, Haoye Zhang, Hongzhang Liu, Yuan Gong, et al. xbench: Tracking agents productivity scaling with profession-aligned real-world evaluations. *arXiv preprint arXiv:2506.13651*, 2025.
- Patrick Coffee. Ai will soon dominate ad buying, whether marketers like it or not. *The Wall Street Journal*, March 2025. URL <https://www.wsj.com/articles/ai-will-soon-dominate-ad-buying-whether-marketers-like-it-or-not-3d62b754>.

Jacob Eisenstein, Chirag Nagpal, Alekh Agarwal, Ahmad Beirami, Alex D’Amour, DJ Dvijotham, Adam Fisch, Katherine Heller, Stephen Pfohl, Deepak Ramachandran, et al. Helping or herding? reward model ensembles mitigate but do not eliminate reward hacking. *arXiv preprint arXiv:2312.09244*, 2023.

Dyke Ferber, Georg Wölflein, Isabella C Wiest, Marta Ligeró, Srividhya Sainath, Narmin Ghaffari Laleh, Omar SM El Nahhas, Gustav Müller-Franzes, Dirk Jäger, Daniel Truhn, et al. In-context learning enables multimodal large language models to classify cancer pathology images. *Nature Communications*, 15(1): 10104, 2024.

Tanner Fiez, Houssam Nassif, Yu-Cheng Chen, Sergio Gamez, and Lalit Jain. Best of three worlds: Adaptive experimentation for digital marketing in practice. In *Proceedings of the ACM Web Conference 2024*, pages 3586–3597, 2024.

Peter I Frazier. A tutorial on bayesian optimization. *arXiv preprint arXiv:1807.02811*, 2018.

Leo Gao, John Schulman, and Jacob Hilton. Scaling laws for reward model overoptimization. In *International Conference on Machine Learning*, pages 10835–10866. PMLR, 2023.

Tong Geng, Xiliang Lin, and Harikesh S Nair. Online evaluation of audiences for targeted advertising via bandit experiments. In *Proceedings of the AAAI Conference on Artificial Intelligence*, 2020.

Akash Ghosh, Arkadeep Acharya, Sriparna Saha, Vinija Jain, and Aman Chadha. Exploring the frontier of vision-language models: A survey of current methodologies and future directions. *arXiv preprint arXiv:2404.07214*, 2024.

Siyuan Guo, Cheng Deng, Ying Wen, Hechang Chen, Yi Chang, and Jun Wang. Ds-agent: Automated data science by empowering large language models with case-based reasoning. *arXiv preprint arXiv:2402.17453*, 2024.

Jochen Hartmann, Yannick Exner, and Samuel Domdey. The power of generative marketing: Can generative ai create superhuman visual marketing content? *International Journal of Research in Marketing*, 42(1): 13–31, 2025.

John R Hauser, Glen L Urban, Guilherme Liberali, and Michael Braun. Website morphing. *Marketing Science*, 28(2):202–223, 2009.

Neil He, Jiahong Liu, Buze Zhang, Ngoc Bui, Ali Maatouk, Menglin Yang, Irwin King, Melanie Weber, and Rex Ying. Position: Beyond euclidean–foundation models should embrace non-euclidean geometries. *arXiv preprint arXiv:2504.08896*, 2025.

Kelly Hong, Anton Troynikov, and Jeff Huber. Context rot: How increasing input tokens impacts llm performance. Technical report, Chroma, July 2025. URL <https://research.trychroma.com/context-rot>.

- Xinyi Hou, Yanjie Zhao, Shenao Wang, and Haoyu Wang. Model context protocol (mcp): Landscape, security threats, and future research directions. *arXiv preprint arXiv:2503.23278*, 2025.
- Jiaxin Huang, Shixiang Gu, Le Hou, Yuexin Wu, Xuezhi Wang, Hongkun Yu, and Jiawei Han. Large language models can self-improve. In Houda Bouamor, Juan Pino, and Kalika Bali, editors, *Proceedings of the 2023 Conference on Empirical Methods in Natural Language Processing*, pages 1051–1068, Singapore, December 2023. Association for Computational Linguistics. doi:10.18653/v1/2023.emnlp-main.67. URL <https://aclanthology.org/2023.emnlp-main.67/>.
- Kevin Jamieson and Robert Nowak. Best-arm identification algorithms for multi-armed bandits in the fixed confidence setting. In *2014 48th annual conference on information sciences and systems (CISS)*, pages 1–6. IEEE, 2014.
- Tijmen Jansen, Mark Heitmann, Martin Reisenbichler, and David A Schweidel. Automated alignment: Engaging customers with visual generative ai. *Available at SSRN 4656622*, 2024.
- Yixing Jiang, Jeremy Irvin, Ji Hun Wang, Muhammad Ahmed Chaudhry, Jonathan H Chen, and Andrew Y Ng. Many-shot in-context learning in multimodal foundation models. *arXiv preprint arXiv:2405.09798*, 2024.
- Garrett A Johnson. Inferno: A guide to field experiments in online display advertising. *Journal of economics & management strategy*, 32(3):469–490, 2023.
- Omar Khattab, Keshav Santhanam, Xiang Lisa Li, David Hall, Percy Liang, Christopher Potts, and Matei Zaharia. Demonstrate-search-predict: Composing retrieval and language models for knowledge-intensive NLP. *arXiv preprint arXiv:2212.14024*, 2022.
- Omar Khattab, Arnav Singhvi, Paridhi Maheshwari, Zhiyuan Zhang, Keshav Santhanam, Sri Vardhamanan, Saiful Haq, Ashutosh Sharma, Thomas T Joshi, Hanna Moazam, et al. Dspy: Compiling declarative language model calls into self-improving pipelines. *arXiv preprint arXiv:2310.03714*, 2023.
- Ron Kohavi, Diane Tang, and Ya Xu. *Trustworthy online controlled experiments: A practical guide to a/b testing*. Cambridge University Press, 2020.
- Mingze Kong, Zhiyong Wang, Yao Shu, and Zhongxiang Dai. Meta-prompt optimization for llm-based sequential decision making, 2025. URL <https://arxiv.org/abs/2502.00728>.
- Harrison Lee, Samrat Phatale, Hassan Mansoor, Thomas Mesnard, Johan Ferret, Kellie Lu, Colton Bishop, Ethan Hall, Victor Carbune, Abhinav Rastogi, et al. Rlaif vs. rlhf: Scaling reinforcement learning from human feedback with ai feedback. *arXiv preprint arXiv:2309.00267*, 2023.
- Ang Li, Haozhe Chen, Hongseok Namkoong, and Tianyi Peng. Llm generated persona is a promise with a catch. *arXiv preprint arXiv:2503.16527*, 2025a.

- Yafu Li, Xuyang Hu, Xiaoye Qu, Linjie Li, and Yu Cheng. Test-time preference optimization: On-the-fly alignment via iterative textual feedback. *arXiv preprint arXiv:2501.12895*, 2025b.
- Aixin Liu, Bei Feng, Bing Xue, Bingxuan Wang, Bochao Wu, Chengda Lu, Chenggang Zhao, Chengqi Deng, Chenyu Zhang, Chong Ruan, et al. Deepseek-v3 technical report. *arXiv preprint arXiv:2412.19437*, 2024a.
- Tennison Liu, Nicolás Astorga, Nabeel Seedat, and Mihaela van der Schaar. Large language models to enhance bayesian optimization. In *The Twelfth International Conference on Learning Representations*, 2024b.
- Yantao Liu, Zijun Yao, Rui Min, Yixin Cao, Lei Hou, and Juanzi Li. Pairjudge rm: Perform best-of-n sampling with knockout tournament, 2025. URL <https://arxiv.org/abs/2501.13007>.
- Josipa Majic. Vcs wake up to vibe marketing: Ai reshaping the \$250 billion industry. *The Wall Street Journal*, 2025. URL <https://www.forbes.com/sites/josipamajic/2025/03/24/vcs-wake-up-to-vibe-marketing-ai-reshaping-the-250-billion-industry/>.
- Linda Mantia, Surojit Chatterjee, and Vivian S. Lee. Designing a successful agentic ai system. *Harvard Business Review*, 2025. URL <https://hbr.org/2025/10/designing-a-successful-agentic-ai-system>. Accessed: 2025-11-01.
- Blake Mason, Lalit Jain, Ardhendu Tripathy, and Robert Nowak. Finding all epsilon-good arms in stochastic bandits. *Advances in Neural Information Processing Systems*, 33:20707–20718, 2020.
- Sidharth Mudgal, Jong Lee, Harish Ganapathy, YaGuang Li, Tao Wang, Yanping Huang, Zhifeng Chen, Heng-Tze Cheng, Michael Collins, Trevor Strohman, et al. Controlled decoding from language models. *arXiv preprint arXiv:2310.17022*, 2023.
- Preetam Nandy, Divya Venugopalan, Chun Lo, and Shaunak Chatterjee. A/b testing for recommender systems in a two-sided marketplace. *Advances in Neural Information Processing Systems*, 34:6466–6477, 2021.
- Giorgos Nikolaou, Tommaso Mencattini, Donato Crisostomi, Andrea Santilli, Yannis Panagakis, and Emanuele Rodola. Language models are injective and hence invertible. *arXiv preprint arXiv:2510.15511*, 2025.
- Krista Opsahl-Ong, Michael J Ryan, Josh Purtell, David Broman, Christopher Potts, Matei Zaharia, and Omar Khattab. Optimizing instructions and demonstrations for multi-stage language model programs. In Yaser Al-Onaizan, Mohit Bansal, and Yun-Nung Chen, editors, *Proceedings of the 2024 Conference on Empirical Methods in Natural Language Processing*, pages 9340–9366, Miami, Florida, USA, November 2024. Association for Computational Linguistics. doi:10.18653/v1/2024.emnlp-main.525. URL <https://aclanthology.org/2024.emnlp-main.525/>.
- Siru Ouyang, Jun Yan, I Hsu, Yanfei Chen, Ke Jiang, Zifeng Wang, Rujun Han, Long T Le, Samira Daruki, Xiangru Tang, et al. Reasoningbank: Scaling agent self-evolving with reasoning memory. *arXiv preprint arXiv:2509.25140*, 2025.

- Leonard Papenmeier, Matthias Poloczek, and Luigi Nardi. Understanding high-dimensional bayesian optimization. *arXiv preprint arXiv:2502.09198*, 2025.
- Tiany Peng, George Gui, Daniel J Merlau, Grace Jiarui Fan, Malek Ben Sliman, Melanie Brucks, Eric J Johnson, Vicki Morwitz, Abdullah Althenayyan, Silvia Bellezza, et al. A mega-study of digital twins reveals strengths, weaknesses and opportunities for further improvement. *arXiv preprint arXiv:2509.19088*, 2025.
- Jiahao Qiu, Xuan Qi, Hongru Wang, Xinzhe Juan, Yimin Wang, Zelin Zhao, Jiayi Geng, Jiacheng Guo, Peihang Li, Jingzhe Shi, et al. Alita-g: Self-evolving generative agent for agent generation. *arXiv preprint arXiv:2510.23601*, 2025.
- Nils Reimers and Iryna Gurevych. Sentence-bert: Sentence embeddings using siamese bert-networks. *arXiv preprint arXiv:1908.10084*, 2019.
- Daniel Russo. Simple bayesian algorithms for best arm identification. In *Conference on learning theory*, pages 1417–1418. PMLR, 2016.
- Daniel J Russo, Benjamin Van Roy, Abbas Kazerouni, Ian Osband, Zheng Wen, et al. A tutorial on thompson sampling. *Foundations and Trends® in Machine Learning*, 11(1):1–96, 2018.
- Jonathan Scarlett, Ilija Bogunovic, and Volkan Cevher. Lower bounds on regret for noisy gaussian process bandit optimization. In *Conference on Learning Theory*, pages 1723–1742. PMLR, 2017.
- Lennart Schneider, Martin Wistuba, Aaron Klein, Jacek Golebiowski, Giovanni Zappella, and Felice Antonio Merra. Hyperband-based bayesian optimization for black-box prompt selection. In *Forty-second International Conference on Machine Learning*, 2025. URL <https://openreview.net/forum?id=Lm9DXFrCHD>.
- Eric M Schwartz, Eric T Bradlow, and Peter S Fader. Customer acquisition via display advertising using multi-armed bandit experiments. *Marketing Science*, 36(4):500–522, 2017.
- Lin Shi, Chiyu Ma, Wenhua Liang, Xingjian Diao, Weicheng Ma, and Soroush Vosoughi. Judging the judges: A systematic study of position bias in llm-as-a-judge, 2025. URL <https://arxiv.org/abs/2406.07791>.
- David Silver and Richard S Sutton. Welcome to the era of experience. *Google AI*, 1, 2025.
- David Simchi-Levi and Chonghuan Wang. Multi-armed bandit experimental design: Online decision-making and adaptive inference. In *International Conference on Artificial Intelligence and Statistics*, pages 3086–3097. PMLR, 2023.
- Joykirat Singh, Subhabrata Dutta, and Tanmoy Chakraborty. Mechanistic behavior editing of language models, 2025.

- Charlie Snell, Jaehoon Lee, Kelvin Xu, and Aviral Kumar. Scaling llm test-time compute optimally can be more effective than scaling model parameters. *arXiv preprint arXiv:2408.03314*, 2024.
- Dilara Soylu, Christopher Potts, and Omar Khattab. Fine-tuning and prompt optimization: Two great steps that work better together, 2024. URL <https://arxiv.org/abs/2407.10930>.
- Niranjan Srinivas, Andreas Krause, Sham M Kakade, and Matthias W Seeger. Information-theoretic regret bounds for gaussian process optimization in the bandit setting. *IEEE transactions on information theory*, 58(5):3250–3265, 2012.
- Shangyin Tan, Lakshya A Agrawal, Arnav Singhvi, Liheng Lai, Michael J Ryan, Dan Klein, Omar Khattab, Koushik Sen, and Matei Zaharia. Langprobe: a language programs benchmark, 2025. URL <https://arxiv.org/abs/2502.20315>.
- Eric Tang, Bangding Yang, and Xingyou Song. Understanding LLM embeddings for regression. *Transactions on Machine Learning Research*, 2025. ISSN 2835-8856. URL <https://openreview.net/forum?id=Wt6Iz5XNIO>.
- Olivier Toubia, George Z Gui, Tianyi Peng, Daniel J Merlau, Ang Li, and Haozhe Chen. Twin-2k-500: A dataset for building digital twins of over 2,000 people based on their answers to over 500 questions. *arXiv preprint arXiv:2505.17479*, 2025.
- Roman Vershynin. *High-dimensional probability: An introduction with applications in data science*, volume 47. Cambridge university press, 2018.
- Wenjia Wang, Xiaowei Zhang, and Lu Zou. Regret optimality of gp-ucb. *arXiv preprint arXiv:2312.01386*, 2023.
- Wenxiao Wang, Priyatham Kattakinda, and Soheil Feizi. Maestro: Joint graph & config optimization for reliable ai agents. *arXiv preprint arXiv:2509.04642*, 2025.
- Justin Whitehouse, Aaditya Ramdas, and Steven Z Wu. On the sublinear regret of gp-ucb. *Advances in Neural Information Processing Systems*, 36:35266–35276, 2023.
- Thaddäus Wiedemer, Yuxuan Li, Paul Vicol, Shixiang Shane Gu, Nick Matarese, Kevin Swersky, Been Kim, Priyank Jaini, and Robert Geirhos. Video models are zero-shot learners and reasoners, 2025. URL <https://arxiv.org/abs/2509.20328>.
- James Wilson, Frank Hutter, and Marc Deisenroth. Maximizing acquisition functions for bayesian optimization. *Advances in neural information processing systems*, 31, 2018.
- Chengrun Yang, Xuezhi Wang, Yifeng Lu, Hanxiao Liu, Quoc V. Le, Denny Zhou, and Xinyun Chen. Large language models as optimizers, 2024. URL <https://arxiv.org/abs/2309.03409>.

Nicholas Young. *An introduction to Hilbert space*. Cambridge university press, 1988.

Mert Yuksekogul, Federico Bianchi, Joseph Boen, Sheng Liu, Pan Lu, Zhi Huang, Carlos Guestrin, and James Zou. Optimizing generative ai by backpropagating language model feedback. *Nature*, 639:609–616, 2025.

Qizheng Zhang, Changran Hu, Shubhangi Upasani, Boyuan Ma, Fenglu Hong, Vamsidhar Kamanuru, Jay Rainton, Chen Wu, Mengmeng Ji, Hanchen Li, et al. Agentic context engineering: Evolving contexts for self-improving language models. *arXiv preprint arXiv:2510.04618*, 2025.

Yongchao Zhou, Andrei Ioan Muresanu, Ziwen Han, Keiran Paster, Silviu Pitis, Harris Chan, and Jimmy Ba. Large language models are human-level prompt engineers. In *The eleventh international conference on learning representations*, 2022.

A Prompts used for digital marketing

Best-of-N Gradient steps' pairwise tournament prompt for ads.

```
contents = [image1, image2, comparison_prompt]
comparison_prompt =
“You are evaluating two advertisement images for mobile Instagram ads. Which image would be more effective at engaging users and driving
clicks?
RESPOND WITH ONLY THE NUMBER 1 OR 2. NOTHING ELSE.
1 = first image is better
2 = second image is better ”
```

Figure 12: M_{critic} 's pairwise tournament prompt for digital marketing example.

Meta reflection prompt for ads

You are an expert at analyzing visual patterns in advertising performance.

VISUAL ANALYSIS TASK:

I will show you images from the lowest-scoring and highest-scoring ad iterations. Your task is to identify specific visual patterns that distinguish effective from ineffective ads.

VISUAL EXAMPLES – BEST VS WORST PERFORMING:

RANK 1/10 WORST PERFORMING (Score: 2.14/5.0):

Prompt excerpt: <prompt>...

[Image]

RANK 2/10 LOWER HALF (Score: 2.52/5.0):

Prompt excerpt: <prompt>...

[Image]

...

RANK 9/10 UPPER HALF (Score: 3.81/5.0):

Prompt excerpt: <prompt>...

[Image]

RANK 10/10 BEST PERFORMING (Score: 4.15/5.0):

Prompt excerpt: <prompt>...

[Image]

Based on your visual analysis, identify patterns that correlate with higher effectiveness scores:

1. Visual composition and framing differences
2. Lighting conditions and mood variations
3. Color palettes and visual tone patterns
4. Subject positioning and action effectiveness
5. Brand integration approaches
6. Environmental and atmospheric elements

RESPONSE FORMAT:

Provide a structured analysis of visual patterns observed, focusing on what distinguishes high-performing from low-performing ads.

Figure 13: Meta reflection prompt for digital marketing example.

Prompt used for generating prompts for ads generation

Generate a creative, structured and descriptive prompt for a generative AI model (e.g., Imagen) that will produce a brand-aligned, and scroll-stopping advertisement image suitable for an Instagram feed.

A successful prompt must be constructed using the following components and principles:

0. (Most important!) Prompt NEVER includes any description of kids. Kids are not allowed to generate in Imagen 4. Even if creative_brief includes description of "family" or "kids", never include kids in the prompt. Only create adults if humans are included.

1. Key Message (The "Why"): This is the foundational element that guides all other components. It defines the core idea or feeling the ad must communicate. Before writing the rest of the prompt, clearly articulate the message the ad will deliver. This message will act as the "North Star" for all subsequent creative choices. It may be desirable to put the message as the text overlay.

2. Core Components (The "What"):

- This should completely depend on the key message.

- Scene & Environment: Based on the key message, establish a clear, relatable setting that aligns with the brand's lifestyle appeal.

- Action & Narrative: Based on the key message and the scene, describe a dynamic but clear action or interaction to create a sense of a captured moment and tell a micro-story.

- Composition & Framing: Specify the camera shot, angle, and framing (e.g., "low-angle shot," "dynamic medium shot," "close-up on the shoe").

3. Stylistic Qualities (The "How"):

- This should completely depend on the key message and the scene.

- Photography Style: Define the overall aesthetic (e.g., "photorealistic," "cinematic," "professional product photography," "lifestyle action shot").

- Lighting: Be specific about the lighting to set the mood (e.g., "warm golden hour light," "bright morning sun," "dramatic side-lighting").

- Color Palette & Tone: Guide the color scheme and emotional feel (e.g., "vibrant and energetic colors," "empowering and motivational tones," "clean and modern palette").

- Atmosphere & Feeling: Aim to evoke a specific feeling aligned with the brand (e.g., "a feeling of effortless performance," "an atmosphere of vibrant energy," "a sense of supreme comfort").

4. What to Avoid:

- Vagueness: Use specific, descriptive terms instead of "nice" or "good."

- Contradictory Elements: Ensure all elements work together harmoniously.

- Over-stuffing: Focus on a single, clear message without too many competing objects.

5. What to include:

- Logo: create a logo based on creative brief, and naturally place it.

- Text: If you are including a text message, prompt for "negative space for text overlay".

Figure 14: Prompt for generating the prompts for the initial 64 ads.

Prompt for generating the worst-of-64 in GreenBite (plant-based burger patty) ad scenario.

****Key Message:**** To visually communicate the core idea: "Experience the juicy, no-compromise satisfaction of a real burger, made better for you and the planet."

****Image Generation Prompt:**** A dynamic, commercial lifestyle photograph for an Instagram feed ad.

****Core Components:****

- **Scene & Environment:**** A stylish, modern outdoor patio during a late afternoon barbecue. The background is softly blurred, showing contemporary patio furniture, lush green potted plants, and the warm glow of string lights just beginning to turn on.
- **Subject & Action:**** The focal point is a vibrant, stylish woman in her early thirties, captured in a candid moment of pure satisfaction. She is taking a bite of a huge, delicious-looking plant-based burger. Her eyes are closed in bliss, and a small, genuine smile plays on her lips, conveying an authentic "this is amazing" reaction. Juice from the burger is subtly visible on her hand to emphasize its succulence. She is dressed in a casual but chic linen shirt.
- **Product:**** The GreenBite burger is the hero. It's a thick, perfectly seared patty with grill marks, nestled in a glossy brioche bun. It's layered with glistening melted cheddar cheese, crisp green lettuce, a thick slice of ripe red tomato, and caramelized onions spilling out slightly. The burger is partially wrapped in a simple, brown kraft paper sheet which has a small, clean logo on it: "GreenBite" in a modern sans-serif font next to a stylized green leaf.
- **Composition & Framing:**** A medium close-up shot, angled slightly upwards to make the moment feel triumphant and empowering. The camera uses a shallow depth of field, keeping the woman's expression and the burger in sharp focus while the background is beautifully out of focus (bokeh). The composition is balanced, with a clear area of soft background on the upper right side, creating negative space for a text overlay.
- **Stylistic Qualities:****
- **Photography Style:**** High-end, photorealistic commercial food photography with a warm, authentic lifestyle feel. The image should be incredibly sharp and detailed, especially the texture of the burger patty and the fresh ingredients.
- **Lighting:**** Bathed in the warm, dreamy glow of the golden hour. The sunlight comes from the side, creating soft highlights and long, gentle shadows, emphasizing the textures of the food and giving her skin a radiant look.
- **Color Palette & Tone:**** A rich and mouth-watering color palette. Saturated and vibrant, but natural. Warm tones of orange, gold, and red from the sun and the food are balanced by the deep greens of the background foliage and the crispness of the lettuce.
- **Atmosphere & Feeling:**** The image radiates a feeling of guilt-free indulgence, vibrant well-being, and ultimate satisfaction. The atmosphere is confident, positive, and irresistibly appetizing, making the viewer crave that exact experience.

Prompt for generating the best-of-64 in GreenBite (plant-based burger patty) ad scenario.

****1. Key Message (The "Why"):** To visually capture the peak moment of guilt-free indulgence, proving that a plant-based burger can deliver an unbelievably juicy, satisfying, and no-compromise flavor experience identical to a classic beef burger. The text overlay will read: "The No-Compromise Burger."

****2. Core Components (The "What"):**

- **Scene & Environment:**** A vibrant, sun-drenched backyard barbecue scene, shot with a very shallow depth of field. The background is a beautiful, soft-focus bokeh of friends laughing (adults only, 25-40 age range), string lights, and lush greenery, suggesting a warm, sociable atmosphere without distracting from the main subject.
- **Action & Narrative:**** A stylish woman in her early 30s, with a look of pure, blissful satisfaction, is taking the first, epic bite of a burger. Her eyes are closed in enjoyment. Her hands grip the burger firmly but gently. A single, perfect drop of sauce is starting to fall from the side of the burger, caught in mid-air, emphasizing its juiciness.
- **Composition & Framing:**** A dramatic, macro close-up, food photography style. The shot is framed tightly on the lower half of the woman's face and her hands holding the burger, making the burger the undeniable hero. The angle is slightly low to give the burger an epic, monumental feel. The right side of the frame has clean, out-of-focus background elements, creating intentional negative space for a text overlay.

****3. Stylistic Qualities (The "How"):**

- **Photography Style:**** Hyper-realistic, professional commercial food photography. Every detail is rendered with extreme clarity: the char marks on the patty, the condensation on the lettuce, the glistening melt of the plant-based cheese, and the texture of the toasted brioche bun. Shot with a high-end DSLR camera and a macro lens.
- **Lighting:**** Warm, radiant golden hour lighting. The sun acts as a dramatic backlight, creating a halo effect around the burger and the woman's hands, and creating glistening specular highlights on the juicy patty and sauce. The lighting is bright, positive, and makes the food look incredibly appetizing.
- **Color Palette & Tone:**** A mouth-watering and vibrant palette. Rich, savory browns of the seared "GreenBite" patty, deep reds of a ripe tomato slice, vibrant green of crisp lettuce, and a warm golden-yellow of the melted cheese and toasted bun. The overall tone is confident, delicious, and energetic.
- **Atmosphere & Feeling:**** The atmosphere is one of ultimate satisfaction and pure, unadulterated foodie bliss. It feels warm, authentic, and completely satisfying, eliminating any doubt about the quality and taste of the plant-based option.

****4. Inclusions & Details:**

- **The Burger Details:**** The GreenBite patty is thick, with a perfect, glistening sear and visible char marks, looking indistinguishable from high-quality ground beef. It's topped with melting vegan cheddar cheese, a leaf of crisp butter lettuce, a thick slice of heirloom tomato, and a creamy aioli sauce.
- **Logo Placement:**** The burger is partially wrapped at the base with a small square of branded, unbleached butcher paper. The "GreenBite" logo—a simple, modern green leaf icon next to the word "GreenBite" in a clean sans-serif font—is subtly visible on the paper.
- **Negative Space:**** Ensure the composition leaves a clean, uncluttered area of soft-focus background on the right third of the image for text overlay.

Figure 15: Prompts for the best and worst ad among the initial 64 ads.

Prompt for generating the T-BoN ($T = 10$) ad for GreenBite (plant-based burger patty)

Key Message:

"The No-Compromise Burger"—to visually prove that a plant-based burger can be just as juicy, delicious, and satisfying as a traditional beef burger, making it the hero of the ultimate backyard BBQ.

Core Components:

Scene & Environment: A vibrant, meticulously designed modern backyard patio, perfect for a relaxed, aspirational late-afternoon get-together. The background is a soft-focus composition of stylish outdoor furniture, lush green garden plants, and subtly visible, engaged friends enjoying themselves and partaking in the shared experience. Occasional hints of other complementary gourmet side dishes or refreshing beverages on the blurred patio table enhance the sense of a complete, desirable BBQ experience, creating a rich, warm, and inviting social atmosphere.

Action & Narrative: A pair of adult hands are holding up a perfectly constructed, gourmet-style cheeseburger. The action captures either: (A) a moment of serene, authentic anticipation just before the first bite, with the subject's face (in soft focus) conveying genuine contentment or subtle bliss, possibly with eyes gently closed, savoring the aroma; OR (B) the burger held out slightly towards the camera, inviting the viewer into the experience, with the subject's soft-focus expression conveying a shared, authentic delight or playful 'aha!' moment. The emphasis is on genuine human emotion and connection, avoiding any forced, exaggerated, or unnatural expressions (especially if a bite is implied). A single, glistening drop of rich, savory juice is visible, about to fall from the patty, powerfully emphasizing its irresistible succulence and indulgent quality without appearing messy. **Central Subject:** The star of the image is the GreenBite burger. It's a thick, plant-based patty with a deeply browned, flawlessly seared crust and visible grill marks, looking indistinguishable from premium ground beef. It's topped with a layer of glistening, perfectly melted cheddar cheese, a crisp piece of bright green leaf lettuce, a thick, ruby-red slice of a heirloom tomato, and a few rings of sharp red onion, all between a fluffy, toasted brioche bun. **Composition & Framing:** An enticing, slightly low-angle medium close-up shot where the GreenBite burger is the undeniable hero, prominently filling a significant portion of the frame and drawing the viewer's eye directly to its appetizing qualities. The focus is tack-sharp on the GreenBite patty's seared texture and the glistening juice. The hands holding the burger, and the subject's face (if present), along with the backyard scene, are rendered in a beautiful, soft-focus bokeh, creating a strong emotional connection and aspirational appeal while ensuring the burger remains supremely appetizing. There is significant negative space with soft, blurred greenery in the upper portion of the frame for a text overlay.

Stylistic Qualities:

Photography Style: High-end, photorealistic commercial food photography with a cinematic lifestyle feel. The image should be incredibly crisp, detailed, and textured. **Lighting:** Bathed in the warm, dreamy glow of golden hour sunlight. The light source comes from the side, casting soft shadows that accentuate the burger's shape and highlight the glistening textures of the melted cheese and juicy patty. A slight, elegant lens flare bleeds into the frame, adding to the warm, aspirational feel. **Color Palette & Tone:** Rich, saturated, and mouth-watering. A color palette dominated by the warm browns of the seared patty, the vibrant orange of the cheese, the fresh greens of the lettuce, and the deep reds of the tomato, all set against the warm, earthy tones of the background.

Atmosphere & Feeling: Evokes a powerful feeling of shared satisfaction, vibrant well-being, and guilt-free indulgence. The atmosphere is confidently positive, supremely delicious, and distinctly aspirational, conveying a desirable lifestyle of effortless enjoyment. **Brand Elements:**

Logo: The simple, modern "GreenBite" logo (clean sans-serif font with a subtle leaf element) is integrated prominently yet naturally within the scene. It is elegantly printed on the branded wax paper partially wrapping the bottom of the burger, and also subtly visible on a branded napkin or a stylish sauce bottle on the blurred patio table in the background, reinforcing brand presence contextually within the aspirational setting. * In addition to the physical logo placements, a clean, prominent text overlay of the 'GreenBite' brand name, and optionally a relevant tagline (e.g., 'Believe Your Bite'), should be integrated into the significant negative space in the upper portion of the frame. This overlay should be highly legible and reinforce clear brand recognition without detracting from the visual appeal."

Figure 16: Prompts for T-BoN ($T = 10$)

Prompt for generating the GEPA ($T = 10$) ad for GreenBite (plant-based burger patty)

Key Message:

Visually communicate the "no-compromise" promise of GreenBite by capturing the exact moment of pure, blissful satisfaction of a consumer realizing a plant-based burger can be just as juicy and delicious as its beef counterpart.

Core Components:

Scene & Environment: A vibrant, sun-drenched modern backyard patio during a relaxed get-together of friends in their late 20s and early 30s. The setting is stylish and aspirational, featuring a natural wood deck, comfortable outdoor furniture, festoon string lights, and lush, green potted plants in the background.

Action & Narrative: The central focus is a woman with her eyes open, full of genuine, surprised satisfaction, capturing the peak moment of consumption. Her mouth is wide open, actively biting into the fully-loaded GreenBite burger. The patty is clearly visible within her mouth, emphasizing the powerful 'A-ha!' moment of discovery and the sheer indulgence of the bite, directly communicating the 'no-compromise' promise.

Composition & Framing: Dynamic, slightly low-angle medium shot focusing on the woman and the burger. The burger is the hero; the depth of field is shallow, rendering the juicy, perfectly seared patty, melted plant-based cheddar, crisp lettuce, and glossy brioche bun in hyper-detailed, sharp focus. The background is beautifully out of focus with a pleasing bokeh effect. There is negative space in the upper left corner suitable for a text overlay.

Stylistic Qualities: **Photography Style:** High-end, commercial lifestyle food photography. Polished, authentic, and incredibly photorealistic. Looks like an image from a top-tier food publication. **Lighting:** Bathed in warm, cinematic golden hour sunlight. The light creates long, soft shadows and a beautiful, inviting glow, highlighting the textures of the food. Crucially, integrate a strong, warm sun flare or haze into the scene, creating a dramatic, aspirational glow that enhances the sense of satisfaction and makes the overall atmosphere feel more vibrant and special. **Color Palette & Tone:** Rich, warm, and saturated colors. Deep browns of the seared patty, vibrant greens of the lettuce and surrounding plants, warm yellows and oranges from the cheese and sunlight. The overall tone is confident, energetic, and mouth-watering.

Atmosphere & Feeling: A powerful feeling of guilt-free indulgence and vibrant satisfaction. The atmosphere is warm, happy, and effortlessly cool, capturing the joy of sharing great food with friends. **Inclusions:**

Logo: Ensure the 'GreenBite' logo is subtly yet clearly visible on the burger wrapper, or on a small, non-distracting element within the scene, to provide product context without pulling focus from the main action.

Text Overlay: A prominent, clean white text overlay, featuring a strong, benefit-driven headline such as 'THE NO-COMPROMISE BURGER' or 'BEYOND EXPECTATION.', is strategically placed in the negative space (e.g., upper left corner). This headline should be clearly legible, visually impactful, and act as a primary visual element, prioritizing the core message and value proposition over just generic brand reinforcement."

Figure 17: Prompts for GEPA ($T = 10$)

B Scenarios

Below are ten ad campaign scenarios with creative briefs, outlining the strategic and creative direction for each experimental scenario. The selected campaigns cover a diverse range of products across distinct categories. Each campaign addresses a unique consumer need—whether related to sustainability, luxury, technology, or lifestyle—ensuring comprehensive coverage of various market segments. From environmentally-conscious millennials to affluent, experience-driven travelers, the approach accounts for the full spectrum of consumer interests. By focusing on different consumer needs, the structure enables a holistic marketing strategy that captures both niche and broad demands, providing a well-rounded framework for the study.

B.1 Scenario 1: GreenBite Plant-Based Burger

- **Product:** "GreenBite," a new plant-based burger patty.
- **Background:** The market for plant-based food is growing, but many consumers remain skeptical about taste, believing they must sacrifice flavor for health.
- **The Challenge:** Convince flexitarians that GreenBite offers the juicy, satisfying experience of a traditional beef burger with no compromise.
- **Core Insight:** Consumers want to eat better for themselves and the planet, but they fear it means giving up the foods they love.
- **Single-Minded Proposition (SMP):** The delicious, no-compromise burger experience that's better for you and the planet.
- **Reasons to Believe (RTB):** Made with savory pea protein; sears and tastes like real beef; free of soy and GMOs.
- **Desired Response: Think:** "I can finally have a plant-based burger that tastes like the real thing.", **Feel:** Satisfied, vibrant, and guilt-free. **Do:** Purchase GreenBite for their next barbecue.
- **Brand Personality & Tone:** Positive, confident, and mouth-watering.

B.2 Scenario 2: AuraSonics X1 Earbuds

- **Product:** "AuraSonics X1," high-end, noise-canceling wireless earbuds.
- **Background:** The rise of hybrid work and urban density has increased daily auditory overload, making focus a precious commodity.
- **The Challenge:** Cut through the saturated audio market by positioning the X1 not as a gadget, but as an essential tool for mental clarity.
- **Core Insight:** In a world of constant noise, true luxury is the ability to control your own soundscape.

- **Single-Minded Proposition (SMP):** AuraSonics X1 creates a personal sanctuary for focus and immersion.
- **Reasons to Believe (RTB):** Adaptive Active Noise Cancellation; studio-quality audio; all-day battery life; minimalist aluminum design.
- **Desired Response: Think:** "This is the solution I need to escape the daily chaos." **Feel:** Calm, empowered, and sophisticated. **Do:** Visit the website to learn more.
- **Brand Personality & Tone:** Minimalist, intelligent, and calm.

B.3 Scenario 3: Odyssey E-SUV

- **Product:** The "Odyssey E-SUV," a new all-electric family SUV.
- **Background:** Many families want to switch to electric vehicles but are concerned about sacrificing space, safety, and range for sustainability.
- **The Challenge:** Position the Odyssey E-SUV as the first EV that meets all the practical and adventurous needs of a modern family, making the switch to electric feel like an upgrade, not a compromise.
- **Single-Minded Proposition (SMP):** The future of family adventure is here: all-electric, zero compromise.
- **Reasons to Believe (RTB):** 500km range; top-tier safety rating; spacious three-row seating; all-wheel drive capability.
- **Desired Response: Think:** "An electric car can actually handle my family's active lifestyle." **Feel:** Adventurous, optimistic, and secure. **Do:** Schedule a test drive.
- **Brand Personality & Tone:** Inspiring, capable, and forward-thinking.

B.4 Scenario 4: Oasis Eco-Lodge

- **Product:** "Oasis Eco-Lodge," a secluded, luxury resort operating in harmony with its natural surroundings.
- **Background:** The luxury travel market often equates opulence with excess. A growing segment of affluent travelers seeks experiences that are both exclusive and responsible.
- **The Challenge:** Redefine luxury as a seamless integration with nature, promising an experience that is restorative for both the guest and the environment.
- **Core Insight:** For those who have everything, true luxury is not more things, but a deeper connection to something pure and serene.

- **Single-Minded Proposition (SMP):** Rediscover tranquility in a luxury that respects nature.
- **Reasons to Believe (RTB):** Secluded private bungalows; farm-to-table dining with locally sourced ingredients; carbon-neutral operations.
- **Desired Response: Think:** "This is a truly special escape, not just another five-star hotel." **Feel:** Serene, exclusive, and rejuvenated. **Do:** Book a stay.
- **Brand Personality & Tone:** Elegant, peaceful, and understated.

B.5 Scenario 5: Momentum Digital Banking

- **Product:** "Momentum," a mobile-first banking app for freelancers and the gig economy.
- **Background:** Traditional banks are not built for the fluctuating incomes and unique business needs of self-employed professionals.
- **The Challenge:** Position Momentum as the essential financial co-pilot for the independent worker, simplifying complexity and providing stability.
- **Core Insight:** Freelancers love their freedom but feel anxious about their financial instability. They need a tool that brings order to their financial chaos.
- **Single-Minded Proposition (SMP):** Banking that is as flexible and entrepreneurial as you are.
- **Reasons to Believe (RTB):** Automated tax-saving tools; integrated invoicing and payment tracking; instant business expense categorization.
- **Desired Response: Think:** "Finally, a bank that gets the way I work." **Feel:** Empowered, organized, and financially confident. **Do:** Download the app and open an account.
- **Brand Personality & Tone:** Modern, empowering, and simple.

B.6 Scenario 6: MindGarden Meditation App

- **Product:** "MindGarden," a subscription-based meditation and mindfulness app.
- **Background:** While many are interested in mindfulness for stress-relief, they are often intimidated by the practice, seeing it as difficult or time-consuming.
- **The Challenge:** Make meditation feel accessible and achievable for absolute beginners, removing the barriers of time and perceived difficulty.
- **Core Insight:** People want the benefits of mindfulness but are convinced they don't have the time or ability to practice it correctly.

- **Single-Minded Proposition (SMP):** Find your calm in just 5 minutes a day.
- **Reasons to Believe (RTB):** Guided 5-minute sessions for specific needs (anxiety, focus); progress tracking to build a habit; simple, jargon-free instructions.
- **Desired Response: Think:** "I can do this. 5 minutes is easy." **Feel:** Calm, supported, and hopeful. **Do:** Start a free trial.
- **Brand Personality & Tone:** Gentle, approachable, and encouraging.

B.7 Scenario 7: Aeterno Watch

- **Product:** The "Aeterno," a classic, automatic Swiss-made wristwatch with a heritage design.
- **Background:** In an age of smartwatches that are obsolete in a few years, there is a renewed appreciation for objects with permanence and enduring value.
- **The Challenge:** Reassert the relevance of the classic mechanical watch as a symbol of taste, craftsmanship, and timelessness.
- **Core Insight:** In a disposable world, true status comes from owning something permanent that tells a story.
- **Single-Minded Proposition (SMP):** A legacy on your wrist. Craftsmanship that transcends time.
- **Reasons to Believe (RTB):** Swiss-made automatic movement; sapphire crystal glass; timeless design inspired by 1950s classics.
- **Desired Response: Think:** "This is a beautiful object that I will own forever." **Feel:** Prestigious, sophisticated, and discerning. **Do:** Locate an authorized dealer.
- **Brand Personality & Tone:** Elegant, timeless, and confident.

B.8 Scenario 8: SyncFlow B2B Software

- **Product:** "SyncFlow," a project management and collaboration software platform for remote teams.
- **Background:** Remote work has increased flexibility but also created challenges in team alignment, communication, and project visibility.
- **The Challenge:** Cut through a crowded SaaS market by focusing on the outcome of "effortless collaboration" rather than just listing features.
- **Core Insight:** Managers don't want another tool to manage; they want the feeling of clarity and momentum that comes from a team working in perfect sync.

- **Single-Minded Proposition (SMP):** Bring your remote team together for effortless collaboration and remarkable results.
- **Reasons to Believe (RTB):** Centralized dashboards with real-time project status; integrated communication channels; automated workflows and reporting.
- **Desired Response: Think:** "This could finally solve our remote work chaos and get everyone on the same page." **Feel:** Organized, in control, and successful. **Do:** Sign up for a team demo.
- **Brand Personality & Tone:** Professional, efficient, and innovative.

C Extended experiment results

T-BoN BO										
	Aeterno	Aurasonics	Greenbite	Mindgarden	Momentum	Oasis	Odyssey	Synceflow	Average	
WORST5-OF-N	2.942 (0.025)	2.793 (0.023)	2.706 (0.024)	2.722 (0.024)	2.644 (0.024)	2.839 (0.025)	2.828 (0.025)	2.641 (0.023)	2.739	
Steps	1	3.098 (0.028)	2.813 (0.022)	3.001 (0.027)	2.980 (0.027)	2.799 (0.027)	3.062 (0.028)	2.943 (0.027)	2.927 (0.023)	2.932
	2	3.125 (0.026)	2.969 (0.027)	3.041 (0.026)	2.980 (0.027)	2.907 (0.025)	3.107 (0.026)	2.943 (0.027)	2.927 (0.023)	2.982
	3	3.125 (0.026)	3.041 (0.025)	3.041 (0.026)	2.980 (0.027)	2.907 (0.025)	3.131 (0.019)	3.063 (0.019)	2.927 (0.023)	3.013
	4	3.194 (0.029)	3.041 (0.025)	3.041 (0.026)	3.132 (0.022)	2.907 (0.025)	3.324 (0.028)	3.063 (0.019)	2.927 (0.023)	3.062
	5	3.194 (0.029)	3.041 (0.025)	3.076 (0.026)	3.132 (0.022)	2.907 (0.025)	3.324 (0.028)	3.063 (0.019)	3.127 (0.022)	3.096
	6	3.257 (0.023)	3.041 (0.025)	3.076 (0.026)	3.132 (0.022)	2.907 (0.025)	3.324 (0.028)	3.070 (0.022)	3.127 (0.022)	3.097
	7	3.257 (0.023)	3.104 (0.028)	3.076 (0.026)	3.132 (0.022)	2.907 (0.025)	3.324 (0.028)	3.107 (0.027)	3.127 (0.022)	3.111
	8	3.257 (0.023)	3.104 (0.028)	3.076 (0.026)	3.132 (0.022)	2.913 (0.026)	3.324 (0.028)	3.107 (0.027)	3.127 (0.022)	3.112
	9	3.257 (0.023)	3.104 (0.028)	3.076 (0.026)	3.132 (0.022)	2.926 (0.026)	3.324 (0.028)	3.107 (0.027)	3.127 (0.022)	3.114
	10	3.257 (0.023)	3.104 (0.028)	3.168 (0.025)	3.132 (0.022)	3.024 (0.025)	3.324 (0.028)	3.107 (0.027)	3.127 (0.022)	3.155
BEST-OF-N	2.982 (0.025)	2.934 (0.027)	2.898 (0.025)	2.930 (0.028)	3.030 (0.027)	3.265 (0.022)	2.966 (0.027)	3.086 (0.023)	3.011	

Table 2: Progress of T-BoN BO across 10 optimization steps from its starting point (WORST5-OF-N) and comparison with the BEST-OF-N baseline. Each data point, in the mean (standard error) format, indicates the mean and standard error across 411 personas in the test persona set. The last column, labeled “Average”, reports the averages of the means across the eight scenarios.

GEPA										
	Aeterno	Aurasonics	Greenbite	Mindgarden	Momentum	Oasis	Odyssey	Synceflow	Average	
WORST5-OF-N	2.942 (0.025)	2.793 (0.023)	2.706 (0.024)	2.722 (0.024)	2.644 (0.024)	2.839 (0.025)	2.828 (0.025)	2.641 (0.023)	2.739	
Steps	1	3.036 (0.025)	2.942 (0.025)	3.029 (0.025)	2.841 (0.024)	2.816 (0.024)	3.151 (0.024)	2.915 (0.025)	2.880 (0.025)	2.939
	2	3.036 (0.025)	2.942 (0.025)	3.046 (0.024)	2.945 (0.023)	2.907 (0.023)	3.151 (0.024)	3.071 (0.028)	2.880 (0.025)	2.992
	3	3.036 (0.025)	2.942 (0.025)	3.046 (0.024)	2.945 (0.023)	2.907 (0.023)	3.182 (0.025)	3.088 (0.026)	2.914 (0.018)	3.003
	4	3.138 (0.025)	3.028 (0.022)	3.046 (0.024)	2.954 (0.024)	2.976 (0.026)	3.187 (0.023)	3.088 (0.026)	2.949 (0.028)	3.033
	5	3.138 (0.025)	3.028 (0.022)	3.046 (0.024)	3.012 (0.022)	2.976 (0.026)	3.187 (0.023)	3.088 (0.026)	3.008 (0.026)	3.049
	6	3.157 (0.023)	3.028 (0.022)	3.046 (0.024)	3.012 (0.022)	2.976 (0.026)	3.209 (0.020)	3.088 (0.026)	3.008 (0.026)	3.052
	7	3.157 (0.023)	3.028 (0.022)	3.046 (0.024)	3.068 (0.027)	2.976 (0.026)	3.209 (0.020)	3.088 (0.026)	3.008 (0.026)	3.060
	8	3.157 (0.023)	3.028 (0.022)	3.046 (0.024)	3.068 (0.027)	2.976 (0.026)	3.209 (0.020)	3.088 (0.026)	3.008 (0.026)	3.060
	9	3.157 (0.023)	3.028 (0.022)	3.046 (0.024)	3.068 (0.027)	2.976 (0.026)	3.278 (0.023)	3.088 (0.026)	3.008 (0.026)	3.070
	10	3.157 (0.023)	3.028 (0.022)	3.046 (0.024)	3.068 (0.027)	2.976 (0.026)	3.278 (0.023)	3.088 (0.026)	3.008 (0.026)	3.070
BEST-OF-N	2.982 (0.025)	2.934 (0.027)	2.898 (0.025)	2.930 (0.028)	3.030 (0.027)	3.265 (0.022)	2.966 (0.027)	3.086 (0.023)	3.011	

Table 3: Progress of GEPA across 10 optimization steps from its starting point (WORST5-OF-N) and comparison with the BEST-OF-N baseline. Each data point, in the mean (standard error) format, indicates the mean and standard error across 411 personas in the test persona set. The last column, labeled “Average”, reports the averages of the means across the eight scenarios.

	Odyssey (Electric family SUV)	Oasis (Secluded resort)	Momentum (Mobile banking app)	Aeterno (Luxury watch)	Syncflow (Collaboration tool)
WORST5-OF-64	 Score: 2.828	 Score: 2.839	 Score: 2.644	 Score: 2.942	 Score: 2.641
BEST-OF-64	 Score: 2.966	 Score: 3.265	 Score: 3.030	 Score: 2.982	 Score: 3.086
GEPA (T=10)	 Score: 3.088	 Score: 3.278	 Score: 2.976	 Score: 3.157	 Score: 3.008
T-BoN BO (T=10)	 Score: 3.107	 Score: 3.324	 Score: 3.024	 Score: 3.257	 Score: 3.127

Figure 18: T-BoN BO and baseline’s generated Ad images for five fictional brands: Odyssey electric family SUV (Scenario 3), Oasis eco-lodge (Scenario 4), Momentum Digital Banking (Scenario 5), Aeterno luxury watch (Scenario 7), and SyncFlow B2B software (Scenario 8)

D Proofs

D.1 Auxiliary lemmas

Lemma 3 (Uniform first-order expansion). *Let $g = \nabla\mu(x)$ and $h = \nabla\sigma(x)$. There exist $C > 0$ and $\varepsilon_0 > 0$ such that for all $\varepsilon \in (0, \varepsilon_0]$ and all $u \in \mathbb{R}^d$,*

$$\mu(x + \varepsilon u) = \mu(x) + \varepsilon g^\top u + r_\mu(\varepsilon, u), \quad |r_\mu(\varepsilon, u)| \leq C\varepsilon^2, \quad (21)$$

$$\sigma(x + \varepsilon u) = \sigma(x) + \varepsilon h^\top u + r_\sigma(\varepsilon, u), \quad |r_\sigma(\varepsilon, u)| \leq C\varepsilon^2. \quad (22)$$

Proof. By the mean-value theorem with Lipschitz gradients, for some ξ between x and $x + \varepsilon u$, $\mu(x + \varepsilon u) = \mu(x) + \nabla\mu(\xi)^\top(\varepsilon u)$. Hence $\mu(x + \varepsilon u) = \mu(x) + \varepsilon g^\top u + \varepsilon(\nabla\mu(\xi) - \nabla\mu(x))^\top u$, and $|\nabla\mu(\xi) - \nabla\mu(x)| \leq L_\mu\|\xi - x\| \leq L_\mu\varepsilon$, giving $|r_\mu| \leq L_\mu\varepsilon^2$. The proof for σ is identical with L_σ . Taking $C := \max\{L_\mu, L_\sigma\}$ yields the stated bounds with the same C . \square

Lemma 4 (Max-stability under bounded perturbations). *Let $(f_i)_{i \leq N}$ and $(g_i)_{i \leq N}$ be real arrays. Let $i_f \in \arg \max_i f_i$ and $i_g \in \arg \max_i g_i$. If for some $\Delta \geq 0$,*

$$g_{i_f} \geq f_{i_f} - \Delta \quad \text{and} \quad f_{i_g} \geq g_{i_g} - \Delta, \quad (23)$$

then $g_{i_f} \geq \max_i g_i - \Delta$ and $f_{i_g} \geq \max_i f_i - \Delta$. In particular, $g_{i_f} \geq \max_i g_i - \Delta$ implies that any maximizer of f is a Δ -approximate maximizer of g .

Proof. Since $g_{i_f} \geq f_{i_f} - \Delta = \max_i f_i - \Delta \geq g_{i_g} - \Delta = \max_i g_i - \Delta$, the first claim holds. The second is symmetric. \square

Lemma 5 (Spherical cap coverage). *For $v \in \mathbb{S}^{d-1}$ and $\eta \in (0, 1)$, define $C(v, \eta) := \{u \in \mathbb{S}^{d-1} : v^\top u \geq 1 - \eta\}$. Let $U_1, \dots, U_N \stackrel{i.i.d.}{\sim} \rho$ as above. Then $\max_{i \leq N} v^\top U_i \rightarrow 1$ almost surely as $N \rightarrow \infty$. Moreover, for any deterministic sequence $\eta_N \downarrow 0$ with $N \cdot \rho\{u : v^\top u \geq 1 - \eta_N\} \rightarrow \infty$, we have*

$$\mathbb{P}\left(\max_{i \leq N} v^\top U_i \geq 1 - \eta_N\right) \rightarrow 1. \quad (24)$$

Proof. Let $C(\eta) = \{u \in \mathbb{S}^{d-1} : v^\top u \geq 1 - \eta\}$ be a spherical cap. Since ρ has a density bounded below, $\rho(C(\eta)) \asymp \eta^{\frac{d-1}{2}}$ as $\eta \downarrow 0$. Then $\mathbb{P}(\max_i v^\top U_i < 1 - \eta) = (1 - \rho(C(\eta)))^N \leq \exp(-N\rho(C(\eta)))$. For any fixed $\eta \in (0, 1)$, $\sum_{N \geq 1} \mathbb{P}(\max_i v^\top U_i < 1 - \eta) \leq \sum_{N \geq 1} e^{-N\rho(C(\eta))} < \infty$, so by Borel–Cantelli, $\mathbb{P}(\max_i v^\top U_i < 1 - \eta \text{ i.o.}) = 0$. Intersecting over a countable sequence $\eta_m \downarrow 0$ yields $\max_{i \leq N} v^\top U_i \rightarrow 1$ almost surely. Choosing $\eta_N \downarrow 0$ so that $N\rho(C(\eta_N)) \rightarrow \infty$ yields the result, and taking $\eta = \eta_N \rightarrow 0$ proves the first statement. \square

Lemma 6 (Near-maximum coupling in a thin band). *Let $M_N = \max_i \xi_i$ and define $v_N := (g + M_N h) / \|g + M_N h\|$. Also, $S_i := a_i + b_i M_N$, $Y_i^{(0)} := a_i + b_i \xi_i$, $b_i := \sigma(x) + \varepsilon h^\top U_i$. Fix any sequence $c_N \uparrow \infty$ with*

$c_N/q_N \rightarrow 0$ and set $\delta_N := c_N/q_N$. Then with probability $\rightarrow 1$ there exists an index j such that

$$\xi_j \geq M_N - \delta_N \quad \text{and} \quad v_N^\top U_j \geq 1 - \eta_N, \quad (25)$$

whenever $\eta_N \downarrow 0$ satisfies

$$N \mathbb{P}(\xi \geq M_N - \delta_N) \rho\{u : v_N^\top u \geq 1 - \eta_N\} \rightarrow \infty. \quad (26)$$

Moreover, for this j ,

$$S_j - Y_j^{(0)} = b_j(M_N - \xi_j) \leq b_{\max} \delta_N. \quad (27)$$

Proof. Define $p_{\text{cap},N} := \rho\{u : v_N^\top u \geq 1 - \eta_N\}$ and the event

$$E_N := \{M_N \geq q_N - \delta_N\}. \quad (28)$$

By Lemma 1, $M_N - q_N \rightarrow 0$ in probability and $\delta_N \rightarrow 0$, hence $\mathbb{P}(E_N) \rightarrow 1$.

Set the deterministic threshold $t_N := q_N - 2\delta_N$. On E_N we have $M_N - \delta_N \geq q_N - 2\delta_N = t_N$, hence by monotonicity of the tail,

$$\mathbb{P}(\xi \geq t_N) \geq \mathbb{P}(\xi \geq M_N - \delta_N) \quad \text{on } E_N. \quad (29)$$

Let

$$K_N := \sum_{i=1}^N \mathbf{1}\{\xi_i \geq t_N\} \sim \text{Binomial}(N, p_N), \quad p_N := \mathbb{P}(\xi \geq t_N). \quad (30)$$

A Chernoff bound gives

$$\mathbb{P}\left(K_N < \frac{1}{2}Np_N\right) \leq \exp\left(-\frac{1}{8}Np_N\right). \quad (31)$$

Consider

$$L_N := \sum_{i=1}^N \mathbf{1}\{\xi_i \geq t_N\} \mathbf{1}\{v_N^\top U_i \geq 1 - \eta_N\}. \quad (32)$$

Conditional on $\{\xi_i\}_{i=1}^N$ (and hence on K_N and v_N), the variables $\{\mathbf{1}\{v_N^\top U_i \geq 1 - \eta_N\}\}_{i=1}^N$ are i.i.d. Bernoulli($p_{\text{cap},N}$) and independent of $\{\xi_i\}$. Therefore,

$$L_N \mid \{\xi_i\} \sim \text{Binomial}(K_N, p_{\text{cap},N}), \quad \mathbb{P}(L_N = 0 \mid \{\xi_i\}) = (1 - p_{\text{cap},N})^{K_N} \leq \exp(-K_N p_{\text{cap},N}). \quad (33)$$

We now bound $\mathbb{P}(L_N = 0)$ by splitting on $\{K_N \geq \frac{1}{2}Np_N\}$ and E_N :

$$\begin{aligned}
\mathbb{P}(L_N = 0) &\leq \mathbb{E}\left[\exp(-K_N p_{\text{cap},N}) \mathbf{1}_{\{K_N \geq \frac{1}{2}Np_N\} \cap E_N}\right] + \mathbb{P}\left(K_N < \frac{1}{2}Np_N\right) + \mathbb{P}(E_N^c) \\
&\leq \mathbb{E}\left[\exp(-\frac{1}{2}Np_N p_{\text{cap},N}) \mathbf{1}_{E_N}\right] + \exp(-\frac{1}{8}Np_N) + o(1) \\
&\leq \mathbb{E}\left[\exp(-\frac{1}{2}Np_N p_{\text{cap},N})\right] + \exp(-\frac{1}{8}Np_N) + o(1).
\end{aligned} \tag{34}$$

On E_N , (29) yields $p_N \geq \mathbb{P}(\xi \geq M_N - \delta_N)$. By the lemma's hypothesis,

$$Z_N := Np_N p_{\text{cap},N} \geq N \mathbb{P}(\xi \geq M_N - \delta_N) p_{\text{cap},N} \xrightarrow{P} \infty.$$

Since $0 \leq e^{-\frac{1}{2}Z_N} \leq 1$, for any fixed $T > 0$,

$$\mathbb{E}\left[e^{-\frac{1}{2}Z_N}\right] \leq e^{-\frac{1}{2}T} + \mathbb{P}(Z_N \leq T) \longrightarrow e^{-\frac{1}{2}T}.$$

Letting $T \rightarrow \infty$ gives $\mathbb{E}[e^{-\frac{1}{2}Z_N}] \rightarrow 0$. Moreover, $Z_N \leq Np_N$ since $p_{\text{cap},N} \leq 1$. If Np_N were bounded along a subsequence, then Z_N would be bounded along that subsequence, contradicting $Z_N \xrightarrow{P} \infty$. Hence $Np_N \rightarrow \infty$, so $\exp(-\frac{1}{8}Np_N) \rightarrow 0$. Therefore the second term in (34) vanishes, and $\mathbb{P}(L_N = 0) \rightarrow 0$.

Therefore, with probability tending to one there exists j such that $\xi_j \geq t_N$ and $v_N^\top U_j \geq 1 - \eta_N$. Since $t_N \leq M_N - \delta_N$ on E_N , this j also satisfies $\xi_j \geq M_N - \delta_N$. Finally, $S_j - Y_j^{(0)} = b_j(M_N - \xi_j) \leq b_{\max} \delta_N$ holds deterministically by $M_N - \xi_j \leq \delta_N$ and the definition of b_{\max} . \square

D.2 Proof of Theorem 2

Proof.

By Lemma 3,

$$\begin{aligned}
Y_i &= \mu(x) + \varepsilon g^\top u_i + r_\mu(\varepsilon, u_i) + (\sigma(x) + \varepsilon h^\top u_i + r_\sigma(\varepsilon, u_i)) \xi_i \\
&= a_i + b_i \xi_i + R_i,
\end{aligned} \tag{35}$$

where $a_i := \mu(x) + \varepsilon g^\top u_i$, $b_i := \sigma(x) + \varepsilon h^\top u_i$, and $R_i := r_\mu(\varepsilon, u_i) + \xi_i r_\sigma(\varepsilon, u_i)$. Then $|R_i| \leq C\varepsilon^2(1 + |\xi_i|)$ for all i . Define $S_i := a_i + b_i M_N$, $b_{\max} := \max_{1 \leq i \leq N} |b_i|$, and $U_i := u_i$.

Now let $Y_i^{(0)} := a_i + b_i \xi_i$ and $i_0 \in \arg \max_i Y_i^{(0)}$. From (35),

$$Y_{i^*} \geq Y_{i_0} \implies Y_{i^*}^{(0)} \geq Y_{i_0}^{(0)} - |R_{i^*}| - |R_{i_0}|.$$

By the bound on R_i and $|\xi_i| \leq M_N := \max_j \xi_j$,

$$Y_{i^*}^{(0)} \geq \max_i Y_i^{(0)} - 2C\varepsilon^2(1 + M_N). \tag{36}$$

Symmetrically, $\max_i Y_i^{(0)} \geq Y_{i^*}^{(0)} \geq \max_i Y_i^{(0)} - 2C\varepsilon^2(1 + M_N)$. By Lemma 4, i^* is a $2C\varepsilon^2(1 + M_N)$ -

approximate maximizer of $Y^{(0)}$.

Now let j be the index from Lemma 6 so that $\xi_j \geq M_N - \delta_N$ and $v_N^\top U_j \geq 1 - \eta_N$. By Lemma 3,

$$\max_{i \leq N} S_i - S_j \leq \varepsilon \|g + M_N h\| (1 - v_N^\top U_j) + 2C\varepsilon^2(1 + M_N) \leq \varepsilon \|g + M_N h\| \eta_N + 2C\varepsilon^2(1 + M_N).$$

Also,

$$S_j - S_{i^*} = (S_j - Y_j^{(0)}) + (Y_j^{(0)} - Y_{i^*}^{(0)}) + (Y_{i^*}^{(0)} - S_{i^*}) \leq b_{\max} \delta_N + 2C\varepsilon^2(1 + M_N) + \underbrace{(Y_{i^*}^{(0)} - S_{i^*})}_{\leq 0},$$

where the last term is ≤ 0 provided $b_i \geq 0$ for all i , which holds by Assumption A4 for $\varepsilon \leq \varepsilon_0 := \sigma(x)/(2\|h\|)$ when $\sigma(x) > 0$ since $b_i = \sigma(x) + \varepsilon h^\top U_i \geq \sigma(x) - \varepsilon \|h\| \geq \frac{1}{2}\sigma(x) > 0$. Therefore,

$$\max_{i \leq N} S_i - S_{i^*} \leq \varepsilon \|g + M_N h\| \eta_N + b_{\max} \delta_N + 4C\varepsilon^2(1 + M_N). \quad (37)$$

Set:

$$\Delta'_N(\varepsilon) := b_{\max} \frac{c_N}{q_N} + 4C\varepsilon^2(1 + M_N).$$

By Lemma 3,

$$S_i = \mu(x) + M_N \sigma(x) + \varepsilon (g + M_N h)^\top u_i + \tilde{r}_i, \quad |\tilde{r}_i| \leq C\varepsilon^2(1 + M_N).$$

Hence for any i ,

$$S_i - S_{i^*} = \varepsilon \|g + M_N h\| (v_N^\top U_i - v_N^\top \hat{u}_N) + (\tilde{r}_i - \tilde{r}_{i^*}),$$

so

$$|(S_i - S_{i^*}) - \varepsilon \|g + M_N h\| (v_N^\top U_i - v_N^\top \hat{u}_N)| \leq 2C\varepsilon^2(1 + M_N). \quad (38)$$

Taking i that attains $\max_i S_i$ and using (37) yields

$$\max_{i \leq N} v_N^\top U_i - v_N^\top \hat{u}_N \leq \eta_N + \frac{\Delta'_N(\varepsilon)}{\varepsilon \|g + M_N h\|}. \quad (39)$$

Thus

$$1 - v_N^\top \hat{u}_N \leq \underbrace{1 - \max_{i \leq N} v_N^\top U_i}_{\rightarrow 0 \text{ a.s. by Lemma 5}} + \eta_N + \frac{\Delta'_N(\varepsilon)}{\varepsilon \|g + M_N h\|}. \quad (40)$$

Assume $\|h\| > 0$ (the $\|h\| = 0$ case is addressed in Remark 1). Using

$$\|g + M_N h\| \geq M_N \|h\| - \|g\|$$

and Lemma 1, $M_N \rightarrow \infty$ and $M_N \asymp q_N$. Also $b_{\max} \leq \sigma(x) + \varepsilon \|h\| + C\varepsilon^2$. Hence

$$\frac{\Delta'_N(\varepsilon)}{\varepsilon \|g + M_N h\|} = O_p\left(\frac{c_N}{\varepsilon q_N^2 \|h\|}\right) + O\left(\frac{\varepsilon}{\|h\|}\right).$$

Choosing, e.g., $c_N = \frac{1}{2} \log \log N$ and any $\eta_N \downarrow 0$ with

$$N e^{c_N} \rho\{u : v_N^\top u \geq 1 - \eta_N\} \rightarrow \infty$$

makes the RHS of (40) equal to $o_p(1) + O(\varepsilon)$ for fixed $\varepsilon > 0$; then let $\varepsilon \downarrow 0$.

With $N \rightarrow \infty$ first and fixed $\varepsilon > 0$, (40) implies $1 - v_N^\top \hat{u}_N \xrightarrow{p} 0$. Then $\varepsilon \downarrow 0$ removes the $O(\varepsilon)$ residual, yielding $v_N^\top \hat{u}_N \xrightarrow{p} 1$. Since $M_N - q_N \rightarrow 0$ in probability by Lemma 1, the unit vectors $v_N = (g + M_N h) / \|g + M_N h\|$ and $\tilde{v}_N := (g + q_N h) / \|g + q_N h\|$ satisfy $\|v_N - \tilde{v}_N\| \rightarrow 0$ in probability. Hence $\hat{u}_N \xrightarrow{p} \tilde{v}_N$, which is the claimed gradient direction of A_{β_N} with $\beta_N = q_N$.

By Lemma 3,

$$A_{\beta_N}(x + \Delta x^{(N)}) = A_{\beta_N}(x) + \varepsilon \nabla A_{\beta_N}(x)^\top \hat{u}_N + O(\varepsilon^2).$$

Write $\nabla A_{\beta_N}(x) = g + q_N h$. Using $\tilde{v}_N^\top \hat{u}_N \xrightarrow{p} 1$ gives $\nabla A_{\beta_N}(x)^\top \hat{u}_N = \|\nabla A_{\beta_N}(x)\| \tilde{v}_N^\top \hat{u}_N = \|\nabla A_{\beta_N}(x)\| (1 - o_p(1))$. Thus $A_{\beta_N}(x + \Delta x^{(N)}) \geq A_{\beta_N}(x) + \varepsilon \|\nabla A_{\beta_N}(x)\| - o_p(\varepsilon)$, as claimed. \square

Remark 1 (Edge cases). (i) If $\|h\| = 0$, then $\nabla A_{\beta_N}(x) = g$ and the direction reduces to $\nabla \mu(x)$. (ii) If $\sigma(x) = 0$ but $\|h\| > 0$, the result holds unchanged; only the linearization constants change. (iii) If $\sigma(x) = 0$ and $\|h\| = 0$, the model is locally deterministic and the problem is degenerate; selection aligns with $\nabla \mu(x)$ or is undefined if $g = 0$.

E GP-UCB and its evaluation efficiency

Setup. Let f be a unknown, black-box function that maps a compact and convex feasible region $\mathcal{D} \subset \mathbb{R}^d$ to \mathbb{R} . At each time t , a sampling algorithm \mathcal{A} selects a point $x_t \in \mathcal{D}$ to evaluate. This selection is adaptive, based on the history of previously chosen points and their observed outcomes. The evaluation at x_t yields a noisy observation $y_t = f(x_t) + \epsilon_t$, where ϵ_t is a random noise term, where $\{\epsilon_t : t = 1, 2, \dots\}$ are independent, sub-Gaussian random variables. The unknown function f is assumed to be an element of a Reproducing Kernel Hilbert Space (RKHS), $\mathcal{N}_\Psi(\mathcal{D})$, induced by a stationary kernel Ψ . Functions within this RKHS possess a specific smoothness property, the nature of which is determined by the kernel used. The space $\mathcal{N}_\Psi(\mathcal{D})$ is endowed with an inner product and is formally defined as the set of functions

$$\mathcal{N}_\Psi(\mathcal{D}) := \left\{ g : \mathcal{D} \mapsto \mathbb{R} \mid g(\mathbf{x}) = \sum_{j=1}^{\infty} c_j \Psi(\mathbf{x} - \mathbf{x}_j), \text{ for } \{c_j\} \subset \mathbb{R} \text{ and } \{\mathbf{x}_j\} \subset \mathcal{D} \text{ such that } \|g\|_{\mathcal{N}_\Psi(\mathcal{D})} < \infty \right\}$$

where the norm is given by: $\|g\|_{\mathcal{N}_\Psi(\mathcal{D})} := \left(\sum_{j,l=1}^{\infty} c_j c_l \Psi(\mathbf{x}_j - \mathbf{x}_l) \right)^{\frac{1}{2}}$. For any two functions $g_1(\mathbf{x}) = \sum_{j=1}^{\infty} a_j \Psi(\mathbf{x} - \mathbf{x}_j)$ and $g_2(\mathbf{x}) = \sum_{l=1}^{\infty} b_l \Psi(\mathbf{x} - \mathbf{x}_l)$ in the space, their inner product is $\langle g_1, g_2 \rangle_{\mathcal{N}_\Psi(\mathcal{D})} := \sum_{j,l=1}^{\infty} a_j b_l \Psi(\mathbf{x}_j - \mathbf{x}_l)$. A key feature of RKHS space is the reproducing property, $\langle g, \Psi(\mathbf{x} - \cdot) \rangle_{\mathcal{N}_\Psi(\mathcal{D})} = g(\mathbf{x})$, which holds for all $\mathbf{x} \in \mathcal{D}$. The norm of the function f in this space is assumed to be bounded such that $\|f\|_{\mathcal{N}_\Psi(\mathcal{D})} \leq B$ for some constant $B > 0$.

The objectives. The performance of \mathcal{A} is often evaluated through two types of regret over a time horizon T . One is *cumulative regret*, defined as

$$\mathcal{R}_C(T; f, \mathcal{A}) := \sum_{t=1}^T \left[\max_{\mathbf{x} \in \mathcal{D}} f(\mathbf{x}) - f(\mathbf{x}_t) \right] \quad (41)$$

The other is *simple regret*, defined as

$$\mathcal{R}_S(T; f, \mathcal{A}) := \max_{\mathbf{x} \in \mathcal{D}} f(\mathbf{x}) - f(\mathbf{x}^{(T)}) \quad (42)$$

where $\mathbf{x}^{(T)}$ is the output of the algorithm \mathcal{A} after taking T function evaluations.

The lower bound. Scarlett et al. [2017] showed that a lower bound exists on the regret of *any* algorithm for $f \in \mathcal{N}_\Psi(\mathcal{D})$. Specifically, for any constant $B > 0$,

$$\inf_{\mathcal{A}} \sup_{\|f\|_{\mathcal{N}_\Psi(\mathcal{D})} \leq B} \mathbb{E} [\mathcal{R}_C(T; f, \mathcal{A})] = \begin{cases} \Omega(T^{\frac{\nu+d}{2\nu+d}}), & \text{for Matérn kernels,} \\ \Omega(T^{\frac{1}{2}} \ln^{\frac{d}{2}}(T)), & \text{for SE kernels.} \end{cases} \quad (43)$$

$$\inf_{\mathcal{A}} \sup_{\|f\|_{\mathcal{N}_{\Psi}(\mathcal{D})} \leq B} T(\epsilon, f, \mathcal{A}) = \begin{cases} \Omega\left(\left(\frac{1}{\epsilon}\right)^{2+d/\nu}\right), & \text{for Matérn kernels,} \\ \Omega\left(\frac{1}{\epsilon^2} \left(\log \frac{1}{\epsilon}\right)^{d/2}\right), & \text{for SE kernels.} \end{cases} \quad (44)$$

where Matérn kernels are defined as

$$\Psi_{\text{M}}(\mathbf{x} - \mathbf{x}') := \frac{1}{\Gamma(\nu)2^{\nu-1}} \left(\frac{2\sqrt{\nu}\|\mathbf{x} - \mathbf{x}'\|_2}{\ell}\right)^{\nu} K_{\nu}\left(\frac{2\sqrt{\nu}\|\mathbf{x} - \mathbf{x}'\|_2}{\ell}\right), \quad \mathbf{x}, \mathbf{x}' \in \mathcal{D} \quad (45)$$

and SE kernels are defined as

$$\Psi_{\text{SE}}(\mathbf{x} - \mathbf{x}') = \exp\left(-\frac{\|\mathbf{x} - \mathbf{x}'\|_2^2}{2\ell^2}\right), \quad \mathbf{x}, \mathbf{x}' \in \mathcal{D} \quad (46)$$

where $\nu > 0$ is the smoothness parameter, $\ell > 0$ is the length-scale parameter, $\Gamma(\cdot)$ is the gamma function, $K_{\nu}(\cdot)$ is the modified Bessel function of the second kind of order ν , and $\|\cdot\|_2$ denotes the Euclidean norm.

GP-UCB algorithm. The Gaussian Process Upper Confidence Bound (GP-UCB) algorithm, introduced in the seminal work of Srinivas et al. [2012], operates from a Bayesian perspective by placing a Gaussian Process (GP) prior on the unknown objective function f . This GP is characterized by a zero-mean function and a symmetric, positive-definite covariance function, or kernel, $k : \mathcal{D} \times \mathcal{D} \mapsto \mathbb{R}$, where $k(\mathbf{x}, \mathbf{x}') = \Psi(\mathbf{x} - \mathbf{x}')$ for all $\mathbf{x}, \mathbf{x}' \in \mathcal{D}$. For any finite set of points $\{\mathbf{x}_1, \dots, \mathbf{x}_t\} \subset \mathcal{D}$, the corresponding function values $(f(\mathbf{x}_1), \dots, f(\mathbf{x}_t))^{\top}$ are assumed to follow a multivariate normal distribution with a zero mean vector and a covariance matrix with entries $[\mathbf{K}_t]_{jl} = k(\mathbf{x}_j, \mathbf{x}_l)$. Under the assumption of independent, zero-mean Gaussian observation noise with variance σ^2 , conditioning the GP prior on a set of observations $\mathbf{D}_t := \{(\mathbf{x}_j, y_j) : j = 1, \dots, t\}$ yields a closed-form posterior distribution. The posterior mean and variance at any point $\mathbf{x} \in \mathcal{D}$ are given by:

$$\mathbb{E}[f(\mathbf{x}) \mid \mathbf{D}_t] = \mathbf{k}_t^{\top}(\mathbf{x}) \left(\mathbf{K}_t + \sigma^2 \mathbf{I}_t\right)^{-1} \mathbf{y}_t, \quad \text{Var}[f(\mathbf{x}) \mid \mathbf{D}_t] = k(\mathbf{x}, \mathbf{x}) - \mathbf{k}_t(\mathbf{x})^{\top} \left(\mathbf{K}_t + \sigma^2 \mathbf{I}_t\right)^{-1} \mathbf{k}_t(\mathbf{x}), \quad (47)$$

where $\mathbf{k}_t(\mathbf{x})$ is the vector of covariances between \mathbf{x} and the observed points, \mathbf{K}_t is the covariance matrix of the observed points, \mathbf{y}_t is the vector of observed values, and \mathbf{I}_t is the identity matrix. Inspired by upper confidence bound methods in the multi-armed bandit literature (Auer et al., 2002), GP-UCB employs an optimistic acquisition strategy to select subsequent evaluation points. At each step t , the next point \mathbf{x}_{t+1} is chosen by maximizing an upper confidence bound on the function's value $\mathbf{x}_{t+1} = \arg \max_{\mathbf{x} \in \mathcal{D}} \left(\mathbb{E}[f(\mathbf{x}) \mid \mathbf{D}_t] + \sqrt{\beta_t \text{Var}[f(\mathbf{x}) \mid \mathbf{D}_t]}\right)$. This acquisition function naturally balances exploitation, driven by the posterior mean $\mathbb{E}[f(\mathbf{x}) \mid \mathbf{D}_t]$, with exploration, driven by the posterior standard deviation $\sqrt{\text{Var}[f(\mathbf{x}) \mid \mathbf{D}_t]}$. The tunable parameter $\beta_t > 0$ explicitly governs this trade-off, making its specification critical to the algorithm's performance.

The evaluation efficiency of GP-UCB. Whitehouse et al. [2023], Wang et al. [2023] showed that GP-UCB Srinivas et al. [2012] upper bound on the cumulative regret of *any* algorithm for $f \in \mathcal{N}_\Psi(\mathcal{D})$ that is almost nearly tight. Specifically, for any constant $B > 0$, the GP-UCB algorithm $\mathcal{A}_{\text{GPUCB}}$ achieves

$$\sup_{\|f\|_{\mathcal{N}_\Psi(\mathcal{D})} \leq B} \mathbb{E} [\mathcal{R}_C(T; f, \mathcal{A}_{\text{GPUCB}})] = \begin{cases} O(T^{\frac{\nu+d}{2\nu+d}}), & \text{for Matérn kernels,} \\ O(T^{\frac{1}{2}} \ln^{\frac{d}{2}}(T)) & \text{for SE kernels.} \end{cases} \quad (48)$$

$$\sup_{\|f\|_{\mathcal{N}_\Psi(\mathcal{D})} \leq B} T(\epsilon, f, \mathcal{A}_{\text{GPUCB}}) = \begin{cases} O\left(\left(\frac{1}{\epsilon}\right)^{2+d/\nu}\right), & \text{for Matérn kernels,} \\ O\left(\frac{1}{\epsilon^2} \cdot \left(\log \frac{1}{\epsilon}\right)^{d+3}\right), & \text{for SE kernels.} \end{cases} \quad (49)$$

Wang et al. [2023]’s approach to proving the regret optimality of GP-UCB follows the two-step framework. The first critical component is to construct a high-probability uniform error bound that quantifies the difference between the true objective function $f(x)$ and its posterior mean estimate $\mu_t(x)$ at any given step t . This bound takes the form $|f(x) - \mu_t(x)| \leq \sqrt{\beta_t} \sigma_t(x)$ for all $x \in \mathcal{D}$, where $\sigma_t(x)$ is the posterior standard deviation and β_t is a carefully chosen exploration parameter. The second component involves bounding the cumulative sum of the instantaneous regrets, which, under the uniform error bound, can be related to the sum of the posterior variances $\sum_{t=1}^T \sigma_{t-1}^2(x_t)$. This sum is, in turn, bounded by the maximal information gain, γ_T . The final regret bound is thus a function of T , β_T , and an upper bound on γ_T . Wang et al. [2023] employs tools from empirical process theory and decomposes the estimation error, $f(x) - \mu_t(x)$, into a bias term and a random error term. By leveraging the connection between Gaussian process regression and kernel ridge regression, along with properties of the Fourier transform for stationary kernels, they show that the bias term is bounded by $\|f\|_{\mathcal{N}_\Psi(\mathcal{D})} \sigma_t(x)$. The more challenging random error term is handled by viewing it as an empirical process indexed by a class of functions and bounding its supremum. They bound the ϵ -entropy of this function class, which allows for a high-probability bound on the random error. With the new uniform error bound, we can select a much smaller, dimension-independent exploration parameter β_t that grows only logarithmically with T . Combining this sharper β_t with the tightest known bounds on the maximal information gain γ_T for Matérn and SE kernels, we can achieve the tight cumulative regret of GP-UCB.